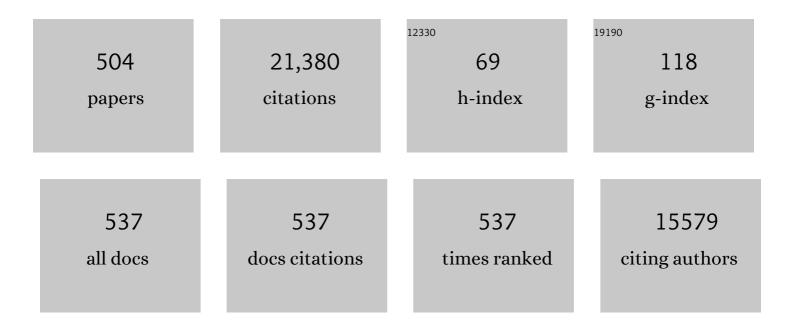
List of Publications by Year in descending order

Source: https://exaly.com/author-pdf/1497707/publications.pdf Version: 2024-02-01



#	Article	IF	CITATION
1	Quantifying global soil carbon losses in response to warming. Nature, 2016, 540, 104-108.	27.8	879
2	Phase II, Open-Label, Single-Arm Trial of Imatinib Mesylate in Patients With Metastatic Melanoma Harboring <i>c-Kit</i> Mutation or Amplification. Journal of Clinical Oncology, 2011, 29, 2904-2909.	1.6	646
3	Performance of the ATLAS trigger system in 2015. European Physical Journal C, 2017, 77, 317.	3.9	489
4	Muon reconstruction performance of the ATLAS detector in proton–proton collision data at \$\$sqrt{s}\$\$ s =13ÂTeV. European Physical Journal C, 2016, 76, 292.	3.9	453
5	Topological cell clustering in the ATLAS calorimeters and its performance in LHC Run 1. European Physical Journal C, 2017, 77, 490.	3.9	325
6	Performance of pile-up mitigation techniques for jets in \$\$pp\$\$ p p collisions at \$\$sqrt{s}=8\$\$. European Physical Journal C, 2016, 76, 581.	3.9	298
7	Luminosity determination in pp collisions at \$\$sqrt{s}\$\$ s = 8 TeV using the ATLAS detector at the LHC. European Physical Journal C, 2016, 76, 653.	3.9	279
8	Measurements of the Higgs boson production and decay rates and coupling strengths using pp collision data at \$\$sqrt{s}=7\$\$ s = 7 and 8ÂTeV in the ATLAS experiment. European Physical Journal C, 2016, 76, 6.	3.9	274
9	Jet energy measurement and its systematic uncertainty in proton–proton collisions at \$\$sqrt{s}=7\$\$ s = 7 ÅTeV with the ATLAS detector. European Physical Journal C, 2015, 75, 17.	3.9	268
10	Performance of the ATLAS Trigger System in 2010. European Physical Journal C, 2012, 72, 1.	3.9	259
11	Search for new phenomena in final states with an energetic jet and large missing transverse momentum in pp collisions at \$\$sqrt{s}=8~\$\$ s = 8 TeV with the ATLAS detector. European Physical lournal C. 2015, 75, 299.	3.9	238

#	Article	IF	CITATIONS
19	Study of the spin and parity of the Higgs boson in diboson decays with the ATLAS detector. European Physical Journal C, 2015, 75, 476.	3.9	174
20	Search for new high-mass phenomena in the dilepton final state using 36 fbâ^'1 of proton-proton collision data at s = 13 \$\$ sqrt{s}=13 \$\$ TeV with the ATLAS detector. Journal of High Energy Physics, 2017, 2017, 1.	4.7	168
21	Measurement of the transverse momentum and \$\$phi ^*_{eta }\$\$ ï• î· â^— distributions of Drell–Yan lepton pairs in proton–proton collisions at \$\$sqrt{s}=8\$\$ s = 8 ÂTeV with the ATLAS detector. European Physical Journal C, 2016, 76, 291.	3.9	154
22	Measurement of the top quark-pair production cross section withÂATLAS in pp collisions at \$sqrt{s}=7\$ ÂTeV. European Physical Journal C, 2011, 71, 1.	3.9	146
23	Jet reconstruction and performance using particle flow with the ATLAS Detector. European Physical Journal C, 2017, 77, 466.	3.9	145
24	Precision measurement and interpretation of inclusive \$\$W^+\$\$ W + , \$\$W^-\$\$ W European Physical Journal C, 2017, 77, 367.	3.9	145
25	ATLAS Run 1 searches for direct pair production of third-generation squarks at the Large Hadron Collider. European Physical Journal C, 2015, 75, 510.	3.9	138
26	Search for dark matter and other new phenomena in events with an energetic jet and large missing transverse momentum using the ATLAS detector. Journal of High Energy Physics, 2018, 2018, 1.	4.7	136
27	Search for doubly charged Higgs boson production in multi-lepton final states with the ATLAS detector using proton–proton collisions at \$\$sqrt{s}=13,ext {TeV}\$\$ s = 13 TeV. European Physical Journal C, 2018, 78, 199.	3.9	132
28	Measurement of the Z/\hat{I}^3 * boson transverse momentum distribution in pp collisions at s = 7 \$\$ sqrt{s}=7 \$\$ TeV with the ATLAS detector. Journal of High Energy Physics, 2014, 2014, 1.	4.7	131
29	ATLAS b-jet identification performance and efficiency measurement with \$\$t{ar{t}}\$\$ events in pp collisions at \$\$sqrt{s}=13\$\$ÂTeV. European Physical Journal C, 2019, 79, 1.	3.9	130
30	Search for electroweak production of supersymmetric particles in final states with two or three leptons at \$\$sqrt{s}=13hbox {TeV}\$\$ s = 13 TeV with the ATLAS detector. European Physical Journal C, 2018, 78, 995.	3.9	125
31	Open-label, Multicenter, Phase II Study of RC48-ADC, a HER2-Targeting Antibody–Drug Conjugate, in Patients with Locally Advanced or Metastatic Urothelial Carcinoma. Clinical Cancer Research, 2021, 27, 43-51.	7.0	125
32	Search for electroweak production of charginos and sleptons decaying into final states with two leptons and missing transverse momentum in \$\$sqrt{s}=13\$\$Â\$\$ext {TeV}\$\$ pp collisions using the ATLAS detector. European Physical Journal C, 2020, 80, 1.	3.9	124
33	Search for the Standard Model Higgs boson produced in association with top quarks and decaying into \$\$varvec{bar{b}}\$\$ b bâ⁻ in \$\$varvec{pp}\$\$ p p collisions at \$\$sqrt{mathbf{s}}= varvec{8{{,mathrm TeV}}}\$\$ s = 8 T e V with the ATLAS detector. European Physical Journal C, 2015, 75, 349.	3.9	123
34	Search for additional heavy neutral Higgs and gauge bosons in the ditau final state produced in 36 fbâ^'1 of pp collisions at s = 13 \$\$ sqrt{s}=13 \$\$ TeV with the ATLAS detector. Journal of High Energy Physics, 2018, 2018, 1.	4.7	116
35	Measurements of top-quark pair differential cross-sections in the lepton+jets channel in pp collisions at \$\$sqrt{s}=8,~{mathrm {TeV}}\$\$ s = 8 TeV using the ATLAS detector. European Physical Journal C, 2016, 76, 538.	3.9	115
36	Safety and clinical activity with an anti-PD-1 antibody JS001 in advanced melanoma or urologic cancer patients. Journal of Hematology and Oncology, 2019, 12, 7.	17.0	113

#	Article	IF	CITATIONS
37	Searches for scalar leptoquarks in pp collisions at \$\$varvec{sqrt{s}}\$\$ s = 8ÂTeV with the ATLAS detector. European Physical Journal C, 2016, 76, 5.	3.9	109
38	Constraints on new phenomena via Higgs boson couplings and invisible decays with the ATLAS detector. Journal of High Energy Physics, 2015, 2015, 1.	4.7	108
39	Search for heavy resonances decaying into WW in the \$\$eu mu u \$\$ e ν μ ν final state in pp collisions at \$\$sqrt{s}=13\$\$ s = 13 \$\$,ext {TeV}\$\$ TeV with the ATLAS detector. European Physical Journal C, 2018, 78, 24.	3.9	108
40	Safety, Efficacy, and Biomarker Analysis of Toripalimab in Previously Treated Advanced Melanoma: Results of the POLARIS-01 Multicenter Phase II Trial. Clinical Cancer Research, 2020, 26, 4250-4259.	7.0	104
41	Measurement of the shape of the boson rapidity distribution for <mml:math xmlns:mml="http://www.w3.org/1998/Math/MathML" display="inline"><mml:mi>p</mml:mi><mml:mover accent="true"><mml:mi>p</mml:mi><mml:mo>Â⁻</mml:mo><mml:mo>â†'</mml:mo><ml:mi>Z< Physical Review D, 2007, 76, .</ml:mi></mml:mover </mml:math 	¢ /ṁ̃ml: mi>	< 101 <mml:mo></mml:mo>
42	Search for heavy ZZ resonances in the \$\$ell ^+ell ^-ell ^+ell ^-\$\$ â"" + â"" - â"" + â"" - and \$\$ell ^+ell ^-u ar{u }\$\$ â"" + â"" - ν ν Â⁻ final states using proton–proton collisions at \$\$sqrt{s}= 13\$\$ s = 13 \$\$ext {TeV}\$\$ TeV with the ATLAS detector. European Physical Journal C, 2018, 78, 293.	3.9	101
43	Constraints on the off-shell Higgs boson signal strength in the high-mass ZZ and WW final states with the ATLAS detector. European Physical Journal C, 2015, 75, 335.	3.9	95
44	Search for new phenomena in events with at least three photons collected in pp collisions at \$\$sqrt{s}\$\$ s = 8 TeV with the ATLAS detector. European Physical Journal C, 2016, 76, 210.	3.9	95
45	Performance of electron and photon triggers in ATLAS during LHC Run 2. European Physical Journal C, 2020, 80, 1.	3.9	93
46	Search for Higgs boson pair production in the \$\$bar{b}bar{b}\$\$ b b Â ⁻ b b Â ⁻ final state from pp collisions at \$\$sqrt{s} = 8\$\$ s = 8 TeVwith the ATLAS detector. European Physical Journal C, 2015, 75, 412.	3.9	90
47	A Phase Ib Study of Pembrolizumab as Second-Line Therapy for Chinese Patients With Advanced or Metastatic Melanoma (KEYNOTE-151). Translational Oncology, 2019, 12, 828-835.	3.7	90
48	Search for the b b \hat{A}^- \$\$ boverline{b} \$\$ decay of the Standard Model Higgs boson in associated (W/Z)H production with the ATLAS detector. Journal of High Energy Physics, 2015, 2015, 1.	4.7	89
49	Electron efficiency measurements with the ATLAS detector using 2012 LHC proton–proton collision data. European Physical Journal C, 2017, 77, 195.	3.9	87
50	Measurement of multi-particle azimuthal correlations in pp, pÂ+ÂPb and low-multiplicity PbÂ+ÂPb collisions with the ATLAS detector. European Physical Journal C, 2017, 77, 428.	3.9	86
51	STAT3/p53 pathway activation disrupts IFN-β–induced dormancy in tumor-repopulating cells. Journal of Clinical Investigation, 2018, 128, 1057-1073.	8.2	86
52	Tislelizumab in Chinese patients with advanced solid tumors: an open-label, non-comparative, phase 1/2 study. , 2020, 8, e000437.		86
53	Search for heavy Majorana neutrinos with the ATLAS detector in pp collisions at \$\$ sqrt{s}=8 \$\$ TeV. Journal of High Energy Physics, 2015, 2015, 1.	4.7	84
54	Muon reconstruction and identification efficiency in ATLAS using the full Run 2 pp collision data set at \$\$\$qrt{s}=13\$\$ TeV. European Physical Journal C, 2021, 81, 1.	3.9	82

#	Article	IF	CITATIONS
55	Measurement of the prompt J/ \$\$psi \$\$ Ï^ pair production cross-section in pp collisions at \$\$sqrt{s} = 8\$\$ s = 8 ÂTeV with the ATLAS detector. European Physical Journal C, 2017, 77, 76.	3.9	81
56	Search for dark matter at \$\$sqrt{s}=13~mathrm{TeV}\$\$ s = 13 TeV in final states containing an energetic photon and large missing transverse momentum with the ATLAS detector. European Physical Journal C, 2017, 77, 393.	3.9	80
57	Search for production of \$\$WW/WZ\$\$ W W / W Z resonances decaying to a lepton, neutrino and jets in \$\$pp\$\$ p p collisions at \$\$sqrt{s}=8\$\$ s = 8 ÂTeV with the ATLAS detector. European Physical Journal C, 2015, 75, 209.	3.9	79
58	Search for lepton-flavour-violating decays of the Higgs and Z bosons with the ATLAS detector. European Physical Journal C, 2017, 77, 70.	3.9	79
59	Search for heavy particles decaying into top-quark pairs using lepton-plus-jets events in proton–proton collisions at \$\$sqrt{s} = 13\$\$ s = 13 \$\$ext {TeV}\$\$ TeV with the ATLAS detector. European Physical Journal C, 2018, 78, 565.	3.9	79
60	Search for high-mass diboson resonances with boson-tagged jets in proton-proton collisions at s = 8 \$\$ sqrt{s}=8 \$\$ TeV with the ATLAS detector. Journal of High Energy Physics, 2015, 2015, 1-39.	4.7	78
61	Electron reconstruction and identification in the ATLAS experiment using the 2015 and 2016 LHC proton–proton collision data at \$\$sqrt{s} = 13\$\$Â\$\$ext {TeV}\$\$. European Physical Journal C, 2019, 79, 1.	3.9	77
62	Angular analysis of B0 d → Kâ^—μ+μâ^' decays in pp collisions at \$\$ sqrt{s}=8 \$\$ TeV with the ATLAS Journal of High Energy Physics, 2018, 2018, 1.	6 detector. 4.7	76
63	Performance of the ATLAS track reconstruction algorithms in dense environments in LHC Run 2. European Physical Journal C, 2017, 77, 673.	3.9	75
64	Measurement of quarkonium production in proton–lead and proton–proton collisions at \$\$5.02~mathrm {TeV}\$\$ 5.02 TeV with the ATLAS detector. European Physical Journal C, 2018, 78, 171.	3.9	75
65	Measurement of the inclusive and dijet cross-sections of b-jets in pp collisions at \$sqrt{s}=7mbox{~TeV}\$ with the ATLAS detector. European Physical Journal C, 2011, 71, 1.	3.9	73
66	Measurement of the photon identification efficiencies with the ATLAS detector using LHC Run-1 data. European Physical Journal C, 2016, 76, 666.	3.9	73
67	Search for squarks and gluinos in final states with jets and missing transverse momentum at \$\$sqrt{s}\$\$ s =13 \$\${mathrm{TeV}}\$ TeV with the ATLAS detector. European Physical Journal C, 2016, 76, 392.	3.9	73
68	Frequent Genetic Aberrations in the CDK4 Pathway in Acral Melanoma Indicate the Potential for CDK4/6 Inhibitors in Targeted Therapy. Clinical Cancer Research, 2017, 23, 6946-6957.	7.0	73
69	Search for supersymmetry at \$\$sqrt{s}=13\$\$ s = 13 ÂTeV in final states with jets and two same-sign leptons or three leptons with the ATLAS detector. European Physical Journal C, 2016, 76, 259.	3.9	72
70	Search for production of vector-like quark pairs and of four top quarks in the lepton-plus-jets final state in pp collisions at s = 8 \$\$ sqrt{s}=8 \$\$ TeV with the ATLAS detector. Journal of High Energy Physics, 2015, 2015, 1.	4.7	71
71	Search for a high-mass Higgs boson decaying to a W boson pair in pp collisions at s = 8 \$\$ sqrt{s}=8 \$\$ TeV with the ATLAS detector. Journal of High Energy Physics, 2016, 2016, 1.	4.7	71
72	<i>MAPK</i> Pathway and <i>TERT</i> Promoter Gene Mutation Pattern and Its Prognostic Value in Melanoma Patients: A Retrospective Study of 2,793 Cases. Clinical Cancer Research, 2017, 23, 6120-6127.	7.0	71

#	Article	IF	CITATIONS
73	Reconstruction of primary vertices at the ATLAS experiment in Run 1 proton–proton collisions at the LHC. European Physical Journal C, 2017, 77, 332.	3.9	71
74	Comparisons of different muscle metabolic enzymes and muscle fiber types in Jinhua and Landrace pigs1. Journal of Animal Science, 2011, 89, 185-191.	0.5	70
75	Identification and energy calibration of hadronically decaying tau leptons with the ATLAS experiment in pp collisions at \$\$sqrt{s}=8\$\$ s = 8 \$\$,hbox {TeV}\$\$ TeV. European Physical Journal C, 2015, 75, 303.	3.9	70
76	Search for resonances in diphoton events at s = 13 \$\$ sqrt{s}=13 \$\$ TeV with the ATLAS detector. Journal of High Energy Physics, 2016, 2016, 1.	4.7	70
77	Early Use of High-Dose Glucocorticoid for the Management of irAE Is Associated with Poorer Survival in Patients with Advanced Melanoma Treated with Anti–PD-1 Monotherapy. Clinical Cancer Research, 2021, 27, 5993-6000.	7.0	70
78	Analysis of <i>mTOR</i> Gene Aberrations in Melanoma Patients and Evaluation of Their Sensitivity to PI3K–AKT–mTOR Pathway Inhibitors. Clinical Cancer Research, 2016, 22, 1018-1027.	7.0	69
79	Search for new resonances in mass distributions of jet pairs using 139 fbâ^'1 of pp collisions at \$\$ sqrt{mathrm{s}} \$\$ = 13 TeV with the ATLAS detector. Journal of High Energy Physics, 2020, 2020, 1.	4.7	68
80	Measurement of charged-particle spectra in Pb+Pb collisions at s N N = 2.76 \$\$ sqrt{s_{mathrm{NN}}=2.76 \$\$ TeV with the ATLAS detector at the LHC. Journal of High Energy Physics, 2015, 2015, 1.	4.7	67
81	Search for direct pair production of a chargino and a neutralino decaying to the 125ÂGeV Higgs boson in \$\$sqrt{varvec{s}} = 8\$\$ s = 8 ÂTeV \$\$varvec{pp}\$\$ p p collisions with the ATLAS detector. European Physical Journal C, 2015, 75, 208.	3.9	67
82	Search for long-lived charginos based on a disappearing-track signature in pp collisions at \$\$ sqrt{s}=13 \$\$ TeV with the ATLAS detector. Journal of High Energy Physics, 2018, 2018, 1.	4.7	67
83	A search for t t Â ⁻ \$\$ toverline{t} \$\$ resonances using lepton-plus-jets events in proton-proton collisions at s = 8 \$\$ sqrt{s}=8 \$\$ TeV with the ATLAS detector. Journal of High Energy Physics, 2015, 2015, 1.	4.7	66
84	A search for pair-produced resonances in four-jet final states at \$\$sqrt{s}=13\$\$ s = 13 \$\$ext {TeV}\$\$ TeV with the ATLAS detector. European Physical Journal C, 2018, 78, 250.	3.9	66
85	Observation and measurements of the production of prompt and non-prompt \$\$varvec{ext {J}uppsi }\$\$ J I^ mesons in association with a \$\$varvec{Z}\$\$ Z boson in \$\$varvec{pp}\$\$ p p collisions at \$\$varvec{sqrt{s}= 8,ext {TeV}}\$\$ s = 8 TeV with the ATLAS detector. European Physical Journal C, 2015, 75, 229.	3.9	64
86	Evidence for the H → b b Â ⁻ \$\$ Ho boverline{b} \$\$ decay with the ATLAS detector. Journal of High Energy Physics, 2017, 2017, 1.	4.7	64
87	Jet energy scale and resolution measured in proton–proton collisions at \$\$sqrt{s}=13\$\$ÂTeV with the ATLAS detector. European Physical Journal C, 2021, 81, 1.	3.9	64
88	Measurement of the differential cross-sections of prompt and non-prompt production of \$\$J/psi \$\$ J / Ï^ and \$\$psi (2mathrm {S})\$\$ Ï^ (2 S) in pp collisions at \$\$sqrt{s} = 7\$\$ s = 7 and 8ÂTeV with the ATLAS detector. European Physical Journal C, 2016, 76, 283.	3.9	63
89	ldentification of boosted, hadronically decaying W bosons and comparisons with ATLAS data taken at \$\$sqrt{s} = 8\$\$ s = 8 ÂTeV. European Physical Journal C, 2016, 76, 154.	3.9	62
90	Genetic Aberrations in the CDK4 Pathway Are Associated with Innate Resistance to PD-1 Blockade in Chinese Patients with Non-Cutaneous Melanoma. Clinical Cancer Research, 2019, 25, 6511-6523.	7.0	62

#	Article	IF	CITATIONS
91	MNK1/2 inhibition limits oncogenicity and metastasis of KIT-mutant melanoma. Journal of Clinical Investigation, 2017, 127, 4179-4192.	8.2	62
92	Charged-particle distributions at low transverse momentum in \$\$sqrt{s} = 13\$\$ s = 13 ÂTeV pp interactions measured with the ATLAS detector at the LHC. European Physical Journal C, 2016, 76, 502.	3.9	61
93	Performance of algorithms that reconstruct missing transverse momentum in \$\$sqrt{s}\$\$ s = 8 TeV proton–proton collisions in the ATLAS detector. European Physical Journal C, 2017, 77, 241.	3.9	61
94	Prompt and non-prompt \$\$J/psi \$\$ J / Ï^ and \$\$psi (2mathrm {S})\$\$ Ï^ (2 S) suppression at high transverse momentum in \$\$5.02~mathrm {TeV}\$\$ 5.02 TeV Pb+Pb collisions with the ATLAS experiment. European Physical Journal C, 2018, 78, 762.	3.9	61
95	Search for doubly charged scalar bosons decaying into same-sign W boson pairs with the ATLAS detector. European Physical Journal C, 2019, 79, 58.	3.9	61
96	Accidental dark matter: Case in the scale invariant local <mml:math xmlns:mml="http://www.w3.org/1998/Math/MathML" display="inline"><mml:mi>B</mml:mi><mml:mo>â^²</mml:mo><mml:mi>L</mml:mi>model. Physical Review D, 2015, 91, .</mml:math 	4.7	60
97	Summary of the searches for squarks and gluinos using s = 8 \$\$ sqrt{s}=8 \$\$ TeV pp collisions with the ATLAS experiment at the LHC. Journal of High Energy Physics, 2015, 2015, 1.	4.7	60
98	Search for a new resonance decaying to a W or Z boson and a Higgs boson in the \$\$ell ell / ell u / u u + b ar{b}\$\$ â"" â"" / â"" ν / Ĩ½ 1½ + b b Â⁻ final states with the ATLAS detector. European Physical Journal C, 2015, 75, 263.	3.9	60
99	Search for dark matter produced in association with bottom or top quarks in \$\$sqrt{s}=13\$\$s=13ÂTeV pp collisions with the ATLAS detector. European Physical Journal C, 2018, 78, 18.	3.9	60
100	Measurement of longitudinal flow decorrelations in Pb+Pb collisions at \$\$sqrt{s_{ext {NN}}=2.76\$\$ s NN = 2.76 and 5.0. European Physical Journal C, 2018, 78, 142.	3.9	59
101	Search for charged Higgs bosons decaying via H± → τ±ντ in the τ+jets and τ+lepton final states with 36 fb of pp collision data recorded at \$\$ sqrt{s}=13 \$\$ TeV with the ATLAS experiment. Journal of High Energy Physics, 2018, 2018, 1.	â^'1 4.7	59
102	Search for supersymmetry in events containing a same-flavour opposite-sign dilepton pair, jets, and large missing transverse momentum in \$\$sqrt{s}=8\$\$ s = 8 ÂTeV pp collisions with the ATLAS detector. European Physical Journal C, 2015, 75, 318.	3.9	56
103	Fiducial, total and differential cross-section measurements of t-channel single top-quark production in pp collisions at 8ÂTeV using data collected by the ATLAS detector. European Physical Journal C, 2017, 77, 531.	3.9	56
104	Search for charged Higgs bosons decaying into top and bottom quarks at \$\$ sqrt{s}=13 \$\$ TeV with the ATLAS detector. Journal of High Energy Physics, 2018, 2018, 1.	4.7	56
105	Search for direct top squark pair production in events with a \$\$Z\$\$ Z boson, \$\$b\$\$ b -jets and missing transverse momentum in \$\$sqrt{s}=8\$\$ s = 8 TeV \$\$pp\$\$ p p collisions with the ATLAS detector. European Physical Journal C, 2014, 74, 2883.	3.9	55
106	Summary of the ATLAS experiment's sensitivity to supersymmetry after LHC Run 1 — interpreted in the phenomenological MSSM. Journal of High Energy Physics, 2015, 2015, 1.	4.7	55
107	GNAQ and GNA11 mutations occur in 9.5% of mucosal melanoma and are associated with poor prognosis. European Journal of Cancer, 2016, 65, 156-163.	2.8	55
108	Search for pair production of Higgs bosons in the \$\$ boverline{b}boverline{b} \$\$ final state using proton-proton collisions at \$\$ sqrt{s}=13 \$\$ TeV with the ATLAS detector. Journal of High Energy Physics, 2019, 2019, 1.	4.7	55

#	Article	IF	CITATIONS
109	Measurements of fiducial cross-sections for \$\$tar{t}\$\$ t t Â⁻ production with one or two additional b-jets in pp collisions at \$\$sqrt{s}\$\$ s =8 TeVÂusing the ATLAS detector. European Physical Journal C, 2016, 76, 11.	3.9	54
110	Search for Higgs boson pair production in the \$\$gamma gamma WW^*\$\$ γ γ W W â^— channel using \$\$pp\$\$ pp collision data recorded at \$\$sqrt{s}\$\$ s \$\$=13\$\$ = 13 TeV with the ATLAS detector. European Physical Journal C, 2018, 78, 1007.	3.9	53
111	Performance of jet substructure techniques for large-R jets in proton-proton collisions at \$ sqrt{s}=7 \$ TeV using the ATLAS detector. Journal of High Energy Physics, 2013, 2013, 1.	4.7	52
112	Search for lepton-flavour-violating H → μÏ,, decays of the Higgs boson with the ATLAS detector. Journal of High Energy Physics, 2015, 2015, 1.	4.7	52
113	Measurement of the top quark mass in the \$\$tar{t}ightarrow ext{ lepton+jets } \$\$ t t Â ⁻ → lepton+jets and \$\$tar{t}ightarrow ext{ dilepton } \$\$ t t Â ⁻ → dilepton channels using \$\$sqrt{s}=7\$\$ s = 7 Â \$\${mathrm { TeV}}\$\$ TeV ATLAS data. European Physical Journal C, 2015, 75, 330.	3.9	52
114	Search for the direct production of charginos and neutralinos in final states with tau leptons in \$\$sqrt{s} = 13,mathrm{TeV}\$\$ s = 13 TeV pp collisions with the ATLAS detector. European Physical Journal C, 2018, 78, 154.	3.9	52
115	A comprehensive approach to dark matter studies: exploration of simplified top-philic models. Journal of High Energy Physics, 2016, 2016, 1.	4.7	51
116	Search for minimal supersymmetric standard model Higgs Bosons HÂ/ÂA and for a \$\$Z^{prime }\$\$ Z ′ boson in the \$\$au au \$\$ Ï,, Ï,, final state produced in pp collisions at \$\$sqrt{s}= 13\$\$ s = 13 TeV with the ATLAS detector. European Physical Journal C, 2016, 76, 585.	3.9	51
117	Measurement of the charged-particle multiplicity inside jets from \$\$sqrt{s}=8\$\$ s = 8 \$\${mathrm{TeV}}\$\$ TeV App collisions with the ATLAS detector. European Physical Journal C, 2016, 76, 322.	3.9	51
118	Measurement of jet fragmentation in Pb+Pb and pp collisions at \$\$sqrt{{s_mathrm{NN}}} = 2.76\$\$ s NN = 2.76. European Physical Journal C, 2017, 77, 379.	3.9	51
119	Measurement of the azimuthal anisotropy of charged particles produced in \$\$sqrt{s_{_ext {NN}}\$\$ s NN = 5.02ÂTeV Pb+Pb collisions with the ATLAS detector. European Physical Journal C, 2018, 78, 997.	3.9	51
120	Reconstruction of hadronic decay products of tau leptons with the ATLAS experiment. European Physical Journal C, 2016, 76, 295.	3.9	50
121	Search for direct top squark pair production in final states with two leptons in \$\$sqrt{s} = 13\$\$ s = 13 TeV pp collisions with the ATLAS detector. European Physical Journal C, 2017, 77, 898.	3.9	50
122	Search for a new heavy gauge-boson resonance decaying into a lepton and missing transverse momentum in 36 fb \$\$^{-1}\$\$ - 1 of pp collisions at. European Physical Journal C, 2018, 78, 401.	3.9	50
123	Search for heavy neutral leptons in decays of W bosons produced in 13 TeV pp collisions using prompt and displaced signatures with the ATLAS detector. Journal of High Energy Physics, 2019, 2019, 1.	4.7	50
124	Search for invisible decays of a Higgs boson using vector-boson fusion in pp collisions at s = 8 \$\$ sqrt{s}=8 \$\$ TeV with the ATLAS detector. Journal of High Energy Physics, 2016, 2016, 1.	4.7	49
125	Constraints on mediator-based dark matter and scalar dark energy models using \$\$ sqrt{s} \$\$ = 13 TeV pp collision data collected by the ATLAS detector. Journal of High Energy Physics, 2019, 2019, 1.	4.7	49
126	MicroRNA-23a-3p Inhibits Mucosal Melanoma Growth and Progression through Targeting Adenylate Cyclase 1 and Attenuating cAMP and MAPK Pathways. Theranostics, 2019, 9, 945-960.	10.0	49

#	Article	IF	CITATIONS
127	Test of CP invariance in vector-boson fusion production of the Higgs boson using the Optimal Observable method in the ditau decay channel with the ATLAS detector. European Physical Journal C, 2016, 76, 658.	3.9	48
128	Search for top-squark pair production in final states with one lepton, jets, and missing transverse momentum using 36 fbâ"1 of \$\$ sqrt{s}=13 \$\$ TeV pp collision data with the ATLAS detector. Journal of High Energy Physics, 2018, 2018, 1.	4.7	48
129	Measurements of the production cross section of a \$\$Z\$\$ Z boson in association with jets in pp collisions at \$\$sqrt{s} = 13\$\$ s. European Physical Journal C, 2017, 77, 361.	3.9	47
130	Measurement of the top quark mass in the $te {t} e^{t} e^{t} e^{t} e^{t} e^{t} e^{t} e^{t}$. European Physical Journal C, 2019, 79, 1.	3.9	47
131	Prognostic factors for conjunctival melanoma: a study in ethnic Chinese patients. British Journal of Ophthalmology, 2015, 99, 990-996.	3.9	46
132	Study of the rare decays of \$\$B^0_s\$\$ B s 0 and \$\$B^0\$\$ B 0 into muon pairs from data collected during the LHC Run 1 with the ATLAS detector. European Physical Journal C, 2016, 76, 513.	3.9	46
133	Measurement of the Higgs boson coupling properties in the H → ZZâ^— → 4â,," decay channel at \$\$ sqrt{s}=13 TeV with the ATLAS detector. Journal of High Energy Physics, 2018, 2018, 1.	\$\$ 4.7	46
134	Measurement of the photon identification efficiencies with the ATLAS detector using LHC Run 2 data collected in 2015 and 2016. European Physical Journal C, 2019, 79, 1.	3.9	46
135	Search for charged Higgs bosons decaying into a top quark and a bottom quark at \$\$ sqrt{mathrm{s}} \$\$ = 13 TeV with the ATLAS detector. Journal of High Energy Physics, 2021, 2021, 1.	4.7	46
136	Single hadron response measurement and calorimeter jet energy scale uncertainty with the ATLAS detector at the LHC. European Physical Journal C, 2013, 73, 1.	3.9	45
137	Search for supersymmetry at \$sqrt{s}\$ = 8 TeV in final states with jets and two same-sign leptons or three leptons with the ATLAS detector. Journal of High Energy Physics, 2014, 2014, 1.	4.7	45
138	Search for a scalar partner of the top quark in the jets plus missing transverse momentum final state at s = 13 \$\$ sqrt{s}=13 \$\$ TeV with the ATLAS detector. Journal of High Energy Physics, 2017, 2017, 1.	4.7	45
139	Measurement of the inclusive isolated prompt photon cross section in pp collisions at s = 8 \$\$ sqrt{s}=8 \$\$ TeV with the ATLAS detector. Journal of High Energy Physics, 2016, 2016, 1.	4.7	44
140	Search for charged Higgs bosons in the H ± → tb decay channel in pp collisions at s = 8 \$\$ sqrt{s}=8 \$\$ TeV using the ATLAS detector. Journal of High Energy Physics, 2016, 2016, 1.	4.7	43
141	Search for single production of vector-like quarks decaying into Wb in pp collisions at \$\$sqrt{s} = 8 \$\tilde{T}EV with the ATLAS detector. European Physical Journal C, 2016, 76, 442.	3.9	43
142	Search for single top-quark production via flavour-changing neutral currents at 8ÂTeV with the ATLAS detector. European Physical Journal C, 2016, 76, 55.	3.9	43
143	Performance of top-quark and \$\$varvec{W}\$\$ W -boson tagging with ATLAS in Run 2 of the LHC. European Physical Journal C, 2019, 79, 1.	3.9	42
144	Phosphorylation of mTOR and S6RP predicts the efficacy of everolimus in patients with metastatic renal cell carcinoma. BMC Cancer, 2014, 14, 376.	2.6	41

#	Article	IF	CITATIONS
145	Measurement of the \$\${varvec{tar{t}Z}}\$\$ t t Â ⁻ Z and \$\${varvec{tar{t}W}}\$\$ t t Â ⁻ W production cross sections in multilepton final states using 3.2 fb \$\$^{-1}\$\$ - 1 of \$\$varvec{pp}\$\$ p p collisions at \$\$sqrt{s}\$\$ s = 13 TeV with the ATLAS detector. European Physical Journal C, 2017, 77, 40.	3.9	41
146	Measurement of \$\$W^{pm }Z\$\$ production cross sections and gauge boson polarisation in pp collisions at \$\$sqrt{s} = 13~ext {TeV}\$\$ with the ATLAS detector. European Physical Journal C, 2019, 79, 1.	3.9	41
147	Higgs boson production cross-section measurements and their EFT interpretation in the \$\$4ell \$\$ decay channel at \$\$sqrt{s}=\$\$13ÂTeV with the ATLAS detector. European Physical Journal C, 2020, 80, 1.	3.9	41
148	Study of the \$\$B_c^+ ightarrow J/psi D_s^+\$\$ B c + → J / Ï^ D s + and \$\$B_c^+ ightarrow J/psi D_s^{*+}\$\$ B c + → J / Ï^ D s â^— + decays with the ATLAS detector. European Physical Journal C, 2016, 76, 4.	3.9	40
149	Search for heavy resonances decaying into a W or Z boson and a Higgs boson in final states with leptons and b-jets in 36 fbâ''1 of \$\$ sqrt{s}=13 \$\$ TeV pp collisions with the ATLAS detector. Journal of High Energy Physics, 2018, 2018, 1.	4.7	40
150	Measurements of b-jet tagging efficiency with the ATLAS detector using \$\$ toverline{t} \$\$ events at \$\$ sqrt{s}=13 \$\$ TeV. Journal of High Energy Physics, 2018, 2018, 1.	4.7	40
151	RBCK1 promotes p53 degradation via ubiquitination in renal cell carcinoma. Cell Death and Disease, 2019, 10, 254.	6.3	40
152	Search for heavy resonances decaying into a pair of Z bosons in the \$\$ell ^+ell ^-ell '^+ell '^-\$\$ and \$\$ell ^+ell ^-u {{ar{u }}}\$\$ final states using 139 \$\$mathrm {fb}^{-1}\$\$ of proton–proton collisions at \$\$sqrt{s} = 13,\$\$TeV with the ATLAS detector. European Physical Journal C, 2021, 81, 1.	3.9	40
153	Search for flavour-changing neutral current top-quark decays to \$\$varvec{qZ}\$\$ q Z in \$\$varvec{pp}\$\$ p p collision data collected with the ATLAS detector at \$\$varvec{sqrt{s}=8}\$\$ s = 8 ÂTeV. European Physical Journal C, 2016, 76, 12.	3.9	39
154	Measurement of the charge asymmetry in top-quark pair production in the lepton-plus-jets final state in pp collision data at \$\$sqrt{s}=8,mathrm TeV{}\$\$ s = 8 T e. European Physical Journal C, 2016, 76, 87.	3.9	39
155	Search for heavy Majorana or Dirac neutrinos and right-handed W gauge bosons in final states with two charged leptons and two jets at \$\$ sqrt{s}=13 \$\$ TeV with the ATLAS detector. Journal of High Energy Physics, 2019, 2019, 1.	4.7	39
156	Measurement of the double-differential high-mass Drell-Yan cross section in pp collisions at s = 8 \$\$ sqrt{s}=8 \$\$ TeV with the ATLAS detector. Journal of High Energy Physics, 2016, 2016, 1.	4.7	38
157	Search for pair production of vector-like top quarks in events with one lepton, jets, and missing transverse momentum in s = 13 \$\$ sqrt{s}=13 \$\$ TeV pp collisions with the ATLAS detector. Journal of High Energy Physics, 2017, 2017, 1.	4.7	38
158	Search for Higgs boson pair production in the \$\$ upgamma upgamma boverline{b} \$\$ final state with 13 TeV pp collision data collected by the ATLAS experiment. Journal of High Energy Physics, 2018, 2018, 1.	4.7	38
159	Measurements of WH and ZH production in the \$\$H ightarrow bar{b}\$\$ decay channel in pp collisions at \$\$13,ext {Te}ext {V}\$\$ with the ATLAS detector. European Physical Journal C, 2021, 81, 1.	3.9	38
160	Search for bottom squark pair production in proton–proton collisions at \$\$sqrt{s}=13\$\$ s = 13 ÂTeV with the ATLAS detector. European Physical Journal C, 2016, 76, 547.	3.9	37
161	Measurement of the W boson polarisation in \$\$tar{t}\$\$ t t Â⁻ events from pp collisions at \$\$sqrt{s}\$\$ s = 8 TeV in the leptonÂ+Âjets channel with ATLAS. European Physical Journal C, 2017, 77, 264.	3.9	37
162	Search for supersymmetry in final states with missing transverse momentum and multiple b-jets in proton-proton collisions at \$\$ sqrt{s}=13 \$\$ TeV with the ATLAS detector. Journal of High Energy Physics, 2018, 2018, 1.	4.7	37

#	Article	IF	CITATIONS
163	Electron and photon energy calibration with the ATLAS detector using 2015–2016 LHC proton-proton collision data. Journal of Instrumentation, 2019, 14, P03017-P03017.	1.2	37
164	Search for squarks and gluinos in final states with jets and missing transverse momentum using 139 fbâ^`1 of \$\$ sqrt{s} \$\$ = 13 TeV pp collision data with the ATLAS detector. Journal of High Energy Physics, 2021, 2021, 1.	4.7	37
165	Randomized Phase II Study of Bevacizumab in Combination With Carboplatin Plus Paclitaxel in Patients With Previously Untreated Advanced Mucosal Melanoma. Journal of Clinical Oncology, 2021, 39, 881-889.	1.6	37
166	Search for heavy lepton resonances decaying to a Z boson and a lepton in pp collisions at s = 8 \$\$ sqrt{s}=8 \$\$ TeV with the ATLAS detector. Journal of High Energy Physics, 2015, 2015, 1.	4.7	36
167	Search for heavy long-lived multi-charged particles in pp collisions at \$\$sqrt{s}=8\$\$ s = 8 ÂTeV using the ATLAS detector. European Physical Journal C, 2015, 75, 362.	3.9	36
168	Search for pair production of heavy vector-like quarks decaying to high-p T W bosons and b quarks in the lepton-plus-jets final state in pp collisions at s = 13 \$\$ sqrt{s}=13 \$\$ TeV with the ATLAS detector. Journal of High Energy Physics, 2017, 2017, 1.	4.7	36
169	Measurement of flow harmonics correlations with mean transverse momentum in lead–lead and proton–lead collisions atÂ\$\$sqrt{s_{mathrm{NN}} = 5.02~hbox {TeV}\$\$ with the ATLAS detector. European Physical Journal C, 2019, 79, 1.	3.9	36
170	Search for pairs of scalar leptoquarks decaying into quarks and electrons or muons in \$\$ sqrt{s} \$\$ = 13 TeV pp collisions with the ATLAS detector. Journal of High Energy Physics, 2020, 2020, 1.	4.7	36
171	Search for a scalar partner of the top quark in the all-hadronic \$\$t{ar{t}}\$\$ plus missing transverse momentum final state at \$\$sqrt{s}=13\$\$ÂTeV with the ATLAS detector. European Physical Journal C, 2020, 80, 1.	3.9	36
172	Safety, Efficacy, and Biomarker Analysis of Toripalimab in Patients with Previously Treated Advanced Urothelial Carcinoma: Results from a Multicenter Phase II Trial POLARIS-03. Clinical Cancer Research, 2022, 28, 489-497.	7.0	36
173	Measurement of the inclusive jet cross-section in proton-proton collisions at s = 7 \$\$ sqrt{s}=7 \$\$ TeV using 4.5 fbâ^'1 of data with the ATLAS detector. Journal of High Energy Physics, 2015, 2015, 1.	4.7	35
174	Identification and rejection of pile-up jets at high pseudorapidity with the ATLAS detector. European Physical Journal C, 2017, 77, 580.	3.9	35
175	Multifactorial Analysis of Prognostic Factors and Survival Rates Among 706 Mucosal Melanoma Patients. Annals of Surgical Oncology, 2018, 25, 2184-2192.	1.5	34
176	Measurements of top-quark pair differential and double-differential cross-sections in the \$\$ell \$\$+jets channel with pp collisions at \$\$sqrt{s}=13\$\$ TeV using the ATLAS detector. European Physical Journal C, 2019, 79, 1.	3.9	34
177	Search for direct production of electroweakinos in final states with one lepton, missing transverse momentum and a Higgs boson decaying into two b-jets in \$\$pp\$\$ collisions at \$\$sqrt{s}=13\$\$ÂTeV with the ATLAS detector. European Physical Journal C, 2020, 80, 1.	3.9	34
178	Measurement of the angular coefficients in Z-boson events using electron and muon pairs from data taken at s = 8 \$\$ sqrt{s}=8 \$\$ TeV with the ATLAS detector. Journal of High Energy Physics, 2016, 2016, 1.	4.7	33
179	Measurements of ľ^(2S) and X(3872) → J/ľ¨l€ + ï€ â~' production in pp collisions at s = 8 \$\$ sqrt{s}=8 \$\$ TeV with the ATLAS detector. Journal of High Energy Physics, 2017, 2017, 1.	4.7	33
180	Search for pair production of up-type vector-like quarks and for four-top-quark events in final states with multiple b-jets with the ATLAS detector. Journal of High Energy Physics, 2018, 2018, 1.	4.7	33

#	Article	IF	CITATIONS
181	Determination of the strong coupling constant \$\$alpha _mathrm {s}\$\$ α s from transverse energy–energy correlations in multijet events at \$\$sqrt{s} = 8~hbox {TeV}\$\$. European Physical Journal C, 2017, 77, 872.	3.9	32
182	Measurements of the Higgs boson inclusive and differential fiducial cross sections in the 4\$\$ell \$\$ decay channel at \$\$sqrt{s}\$\$ = 13 TeV. European Physical Journal C, 2020, 80, 1.	3.9	32
183	Search for gluinos in events with an isolated lepton, jets and missing transverse momentum at \$\$sqrt{s}\$\$ s = 13 Te V with the ATLAS detector. European Physical Journal C, 2016, 76, 565.	3.9	31
184	A search for prompt lepton-jets in pp collisions at s = 8 \$\$ sqrt{mathrm{s}}=8 \$\$ TeV with the ATLAS detector. Journal of High Energy Physics, 2016, 2016, 1.	4.7	31
185	Measurement of inclusive and differential cross sections in the H → ZZ * → 4ℓ decay channel in pp collisions at s = 13 \$\$ sqrt{s}=13 \$\$ TeV with the ATLAS detector. Journal of High Energy Physics, 2017, 2017, 1.	4.7	31
186	Search for supersymmetry in final states with two same-sign or three leptons and jets using 36 fbâ~'1 of \$\$ sqrt{s}=13 \$\$ TeV pp collision data with the ATLAS detector. Journal of High Energy Physics, 2017, 2017, 1.	4.7	31
187	Search for W W/W Z resonance production in â,,"νqq final states in pp collisions at \$\$ sqrt{s}=13 \$\$ TeV with the ATLAS detector. Journal of High Energy Physics, 2018, 2018, 1.	4.7	31
188	Search for Higgs boson decays to beyond-the-Standard-Model light bosons in four-lepton events with the ATLAS detector at \$\$ sqrt{s}=13 \$\$ TeV. Journal of High Energy Physics, 2018, 2018, 1.	4.7	31
189	Sorafenib in combination with gemcitabine plus cisplatin chemotherapy in metastatic renal collecting duct carcinoma: A prospective, multicentre, single-arm, phase 2 study. European Journal of Cancer, 2018, 100, 1-7.	2.8	31
190	Study of hard double-parton scattering in four-jet events in pp collisions at s = 7 \$\$ sqrt{s}=7 \$\$ TeV with the ATLAS experiment. Journal of High Energy Physics, 2016, 2016, 1.	4.7	30
191	Charged-particle distributions in pp interactions at \$\$sqrt{s}=8 mathrm {, TeV}\$\$ s = 8 TeV measured with the ATLAS detector. European Physical Journal C, 2016, 76, 403.	3.9	30
192	Searches for the Zl̂ ³ decay mode of the Higgs boson and for new high-mass resonances in pp collisions at s = 13 \$\$ sqrt{s}=13 \$\$ TeV with the ATLAS detector. Journal of High Energy Physics, 2017, 2017, 1.	4.7	30
193	Study of $WWgamma WW \hat{1}^3$ and $WZgamma W Z. European Physical Journal C, 2017, 77, 646.$	3.9	30
194	PI3K/AKT/mTOR pathway inhibitors inhibit the growth of melanoma cells with mTOR H2189Y mutations in vitro. Cancer Biology and Therapy, 2018, 19, 584-589.	3.4	30
195	Search for new phenomena in events with same-charge leptons and b-jets in pp collisions at \$\$ sqrt{s}=13 \$\$ TeV with the ATLAS detector. Journal of High Energy Physics, 2018, 2018, 1.	4.7	30
196	Searches for third-generation scalar leptoquarks in \$\$ sqrt{s} \$\$ = 13 TeV pp collisions with the ATLAS detector. Journal of High Energy Physics, 2019, 2019, 1.	4.7	30
197	Evidence for \$\$tar{t}tar{t}\$\$ production in the multilepton final state in proton–proton collisions at \$\$sqrt{s}=13\$\$Â\$\$ext {TeV}\$\$ with the ATLAS detector. European Physical Journal C, 2020, 80, 1.	3.9	30
198	A measurement of the calorimeter response to single hadrons and determination of the jet energy scale uncertainty using LHC Run-1 pp-collision data with the ATLAS detector. European Physical Journal C, 2017, 77, 26.	3.9	29

#	Article	IF	CITATIONS
199	Measurement of the inclusive cross-sections of single top-quark and top-antiquark t-channel production in pp collisions at s = 13 \$\$ sqrt{s}=13 \$\$ TeV with the ATLAS detector. Journal of High Energy Physics, 2017, 2017, 1.	4.7	29
200	Search for dark matter in events with a hadronically decaying vector boson and missing transverse momentum in pp collisions at \$\$ sqrt{s}=13 \$\$ TeV with the ATLAS detector. Journal of High Energy Physics, 2018, 2018, 1.	4.7	29
201	Searches for heavy ZZ and ZW resonances in the â,,"â,,"qq and ν2νqq final states in pp collisions at \$\$ sqrt{s}=13 \$\$ TeV with the ATLAS detector. Journal of High Energy Physics, 2018, 2018, 1.	4.7	29
202	The Clinicopathological and Survival Profiles Comparison Across Primary Sites in Acral Melanoma. Annals of Surgical Oncology, 2020, 27, 3478-3485.	1.5	29
203	Search for heavy diboson resonances in semileptonic final states in pp collisions at \$\$sqrt{s}=13\$\$ÂTeV with the ATLAS detector. European Physical Journal C, 2020, 80, 1.	3.9	29
204	Efficacy and safety of sorafenib versus sunitinib as first-line treatment in patients with metastatic renal cell carcinoma: largest single-center retrospective analysis. Oncotarget, 2016, 7, 27044-27054.	1.8	28
205	Measurement of lepton differential distributions and the top quark mass in $\pm ta^{+}.$ European Physical Journal C, 2017, 77, 804.	3.9	28
206	Measurement of \$\$WW/WZ ightarrow ell u q q^{prime }\$\$ W W / W Z → â,," ν q q ′ production with the hadronically decaying boson reconstructed as one or two jets in pp collisions at \$\$sqrt{s} =8~ext {TeV}\$\$ s = 8 TeV with ATLAS, and constraints on anomalous gauge couplings. European Physical Journal C, 2017, 77, 563.	3.9	28
207	Measurement of the Drell-Yan triple-differential cross section in pp collisions at s = 8 \$\$ sqrt{s}=8 \$\$ TeV. Journal of High Energy Physics, 2017, 2017, 1.	4.7	28
208	Search for the Higgs boson produced in association with a vector boson and decaying into two spin-zero particles in the H → aa → 4b channel in pp collisions at \$\$ sqrt{s}=13 \$\$ TeV with the ATLAS detector. Journal of High Energy Physics, 2018, 2018, 1.	4.7	28
209	TERT copy gain predicts the outcome of high-dose interferon α-2b therapy in acral melanoma. OncoTargets and Therapy, 2018, Volume 11, 4097-4104.	2.0	28
210	Search for long-lived neutral particles in pp collisions at \$\${sqrt{s}} = 13~{ext { TeV}}\$\$ that decay into displaced hadronic jets in the ATLAS calorimeter. European Physical Journal C, 2019, 79, 1.	3.9	28
211	In situ calibration of large-radius jet energy and mass in 13ÂTeVÂproton–proton collisions with the ATLAS detector. European Physical Journal C, 2019, 79, 1.	3.9	28
212	Fluctuations of anisotropic flow in Pb+Pb collisions at \$\$ sqrt{{mathrm{s}}_{mathrm{NN}}} \$\$ = 5.02 TeV with the ATLAS detector. Journal of High Energy Physics, 2020, 2020, 1.	4.7	28
213	Measurement of the transverse momentum distribution of Drell–Yan lepton pairs in proton–proton collisions at \$\$sqrt{s}=13,\$\$TeV with the ATLAS detector. European Physical Journal C, 2020, 80, 1.	3.9	28
214	Search for chargino–neutralino pair production in final states with three leptons and missing transverse momentum in \$\$sqrt{s} = 13\$\$ÂTeV pp collisions with the ATLAS detector. European Physical Journal C, 2021, 81, 1.	3.9	28
215	Search for metastable heavy charged particles with large ionisation energy loss in pp collisions at \$\$varvec{sqrt{s} = 8}\$\$ s = 8 ÂTeV using the ATLAS experiment. European Physical Journal C, 2015, 75, 407.	3.9	27
216	Measurements of top-quark pair differential cross-sections in the \$\$emu \$\$ e μ channel in pp collisions at \$\$sqrt{s} = 13\$\$ s = 13 ÂTeV using the ATLAS detector. European Physical Journal C, 2017, 77, 292.	3.9	27

#	Article	IF	CITATIONS
217	Systemic Immune-Inflammation Index and Circulating T-Cell Immune Index Predict Outcomes in High-Risk Acral Melanoma Patients Treated with High-Dose Interferon. Translational Oncology, 2017, 10, 719-725.	3.7	27
218	Search for new phenomena using the invariant mass distribution of same-flavour opposite-sign dilepton pairs in events with missing transverse momentum in \$\$sqrt{s}=13\$\$ s = 13 Â \$\$ext {Te}ext {V}\$\$ Te pp collisions with the ATLAS detector. European Physical Journal C, 2018, 78, 625.	3.9	27
219	Search for single production of vector-like quarks decaying into Wb in pp collisions at \$\$ sqrt{s} \$\$ = 13 TeV with the ATLAS detector. Journal of High Energy Physics, 2019, 2019, 1.	4.7	27
220	Primary malignant melanoma of the esophagus: A retrospective analysis of clinical features, management, and survival of 76 patients. Thoracic Cancer, 2019, 10, 950-956.	1.9	27
221	Measurement of the top-quark mass in \$\$ toverline{t} \$\$ + 1-jet events collected with the ATLAS detector in pp collisions at \$\$ sqrt{s} \$\$ = 8 TeV. Journal of High Energy Physics, 2019, 2019, 1.	4.7	27
222	Search for pair production of third-generation scalar leptoquarks decaying into a top quark and a ΄-lepton in pp collisions at \$\$ sqrt{s} \$\$ = 13 TeV with the ATLAS detector. Journal of High Energy Physics, 2021, 2021, 1.	4.7	27
223	Measurements of electroweak \$\$Wjj \$\$ W j j production and constraints on anomalous gauge couplings with the ATLAS detector. European Physical Journal C, 2017, 77, 474.	3.9	26
224	Efficacy Evaluation of Imatinib for the Treatment of Melanoma: Evidence From a Retrospective Study. Oncology Research, 2019, 27, 495-501.	1.5	26
225	Search for a heavy Higgs boson decaying into a Z boson and another heavy Higgs boson in the \$\$ell ell bb\$\$ and \$\$ell ell WW\$\$ final states in pp collisions at \$\$sqrt{s}=13\$\$Â\$\$ext {TeV}\$\$ with the ATLAS detector. European Physical Journal C, 2021, 81, 1.	3.9	26
226	NMSSM explanations of the Galactic center gamma ray excess and promising LHC searches. Physical Review D, 2015, 91, .	4.7	25
227	Determination of the top-quark pole mass using t t Â⁻ \$\$ toverline{t} \$\$ + 1-jet events collected with the ATLAS experiment in 7 TeV pp collisions. Journal of High Energy Physics, 2015, 2015, 1.	4.7	25
228	Searches for heavy diboson resonances in pp collisions at s = 13 \$\$ sqrt{s}=13 \$\$ TeV with the ATLAS detector. Journal of High Energy Physics, 2016, 2016, 1.	4.7	25
229	Sorafenib versus sunitinib as first-line treatment agents in Chinese patients with metastatic renal cell carcinoma: the largest multicenter retrospective analysis of survival and prognostic factors. BMC Cancer, 2017, 17, 16.	2.6	25
230	Search for triboson \$\$W^{pm }W^{pm }W^{mp }\$\$ W ± W ± W â^" production in pp collisions at \$\$sqrt{s}=8\$\$ s = 8 Â \$\$ext {TeV}\$\$ TeV with the ATLAS detector. European Physical Journal C, 2017, 77, 141.	3.9	25
231	Mutations in BRAF codons 594 and 596 predict good prognosis in melanoma. Oncology Letters, 2017, 14, 3601-3605.	1.8	25
232	Operation and performance of the ATLAS Tile Calorimeter in RunÂ1. European Physical Journal C, 2018, 78, 987.	3.9	25
233	A strategy for a general search for new phenomena using data-derived signal regions and its application within the ATLAS experiment. European Physical Journal C, 2019, 79, 1.	3.9	25
234	Search for the Higgs boson produced in association with a W boson and decaying to four b-quarks via two spin-zero particles in pp collisions at 13 TeV with the ATLAS detector. European Physical Journal C, 2016, 76, 605.	3.9	24

#	Article	IF	CITATIONS
235	Search for supersymmetry in a final state containing two photons and missing transverse momentum in \$\$varvec{sqrt{s}}\$\$ s Â=Â13ÂTeV \$\$varvec{pp}\$\$. European Physical Journal C, 2016, 76, 517.	3.9	24
236	Iron overload induced by ferric ammonium citrate triggers reactive oxygen species-mediated apoptosis via both extrinsic and intrinsic pathways in human hepatic cells. Human and Experimental Toxicology, 2016, 35, 598-607.	2.2	24
237	Measurement of the cross-section and charge asymmetry of W bosons produced in proton–proton collisions at \$\$sqrt{s}=8~ext {TeV}\$\$ with the ATLAS detector. European Physical Journal C, 2019, 79, 1.	3.9	24
238	Measurement of fiducial and differential \$\$W^+W^-\$\$ production cross-sections at \$\$sqrt{s}=13\$\$ÂTeV with the ATLAS detector. European Physical Journal C, 2019, 79, 1.	3.9	24
239	Search for new non-resonant phenomena in high-mass dilepton final states with the ATLAS detector. Journal of High Energy Physics, 2020, 2020, 1.	4.7	24
240	Pilot Study of CT-Based Radiomics Model for Early Evaluation of Response to Immunotherapy in Patients With Metastatic Melanoma. Frontiers in Oncology, 2020, 10, 1524.	2.8	24
241	Study RC48-C014: Preliminary results of RC48-ADC combined with toripalimab in patients with locally advanced or metastatic urothelial carcinoma Journal of Clinical Oncology, 2022, 40, 515-515.	1.6	24
242	Toripalimab plus axitinib in patients with metastatic mucosal melanoma: 3-year survival update and biomarker analysis. , 2022, 10, e004036.		24
243	A search for high-mass resonances decaying to Ï"+Ï"â^' in pp collisions at \$\$ sqrt{s}=8 \$\$ TeV with the ATLAS detector. Journal of High Energy Physics, 2015, 2015, 1.	4.7	23
244	Search for new phenomena in different-flavour high-mass dilepton final states in pp collisions at \$\$sqrt{s}=13\$\$ s = 13 ÂTev with the ATLAS detector. European Physical Journal C, 2016, 76, 541.	3.9	23
245	Measurement of the inclusive jet cross-sections in proton-proton collisions at s = 8 \$\$ sqrt{s}=8 \$\$ TeV with the ATLAS detector. Journal of High Energy Physics, 2017, 2017, 1.	4.7	23
246	Search for doubly and singly charged Higgs bosons decaying into vector bosons in multi-lepton final states with the ATLAS detector using proton-proton collisions at \$\$ sqrt{mathrm{s}} \$\$ = 13 TeV. Journal of High Energy Physics, 2021, 2021, 1.	4.7	23
247	AtlFast3: The Next Generation of Fast Simulation in ATLAS. Computing and Software for Big Science, 2022, 6, 1.	2.9	23
248	RC48-ADC for metastatic urothelial carcinoma with HER2-positive: Combined analysis of RC48-C005 and RC48-C009 trials Journal of Clinical Oncology, 2022, 40, 4520-4520.	1.6	23
249	Higgs boson mass and complex sneutrino dark matter in the supersymmetric inverse seesaw models. Journal of High Energy Physics, 2014, 2014, 1.	4.7	22
250	Measurement of the electroweak production of dijets in association with a Z-boson and distributions sensitive to vector boson fusion in proton-proton collisions at \$ sqrt{s} \$ = 8 TeV using the ATLAS detector. Journal of High Energy Physics, 2014, 2014, 1.	4.7	22
251	Measurement of the t t Â ⁻ W \$\$ toverline{t}W \$\$ and t t Â ⁻ Z \$\$ toverline{t}Z \$\$ production cross sections in pp collisions at s = 8 \$\$ sqrt{s}=8 \$\$ TeV with the ATLAS detector. Journal of High Energy Physics, 2015, 2015, 1.	4.7	22
252	Study of (W/Z)H production and Higgs boson couplings using H→ W W â^— decays with the ATLAS detector. Journal of High Energy Physics, 2015, 2015, 1.	4.7	22

#	Article	IF	CITATIONS
253	Investigating light NMSSM pseudoscalar states with boosted ditau tagging. Journal of High Energy Physics, 2016, 2016, 1.	4.7	22
254	Search for pair production of heavy vector-like quarks decaying into high-pT W bosons and top quarks in the lepton-plus-jets final state in pp collisions at \$\$ sqrt{s}=13 \$\$ TeV with the ATLAS detector. Journal of High Energy Physics, 2018, 2018, 1.	4.7	22
255	Measurements of top-quark pair spin correlations in the \$\$emu \$\$ channel at \$\$sqrt{s} = 13\$\$ TeV using pp collisions in the ATLAS detector. European Physical Journal C, 2020, 80, 1.	3.9	22
256	Search for new phenomena in events with two opposite-charge leptons, jets and missing transverse momentum in pp collisions at \$\$ sqrt{mathrm{s}} \$\$ = 13 TeV with the ATLAS detector. Journal of High Energy Physics, 2021, 2021, 1.	4.7	22
257	Determination of spin and parity of the Higgs boson in the \$\$WW^*ightarrow e u mu u \$\$ W W â^— → e ν μ ν decay channel with the ATLAS detector. European Physical Journal C, 2015, 75, 231.	3.9	21
258	The performance of the jet trigger for the ATLAS detector during 2011 data taking. European Physical Journal C, 2016, 76, 526.	3.9	21
259	Search for the Standard Model Higgs boson decaying into b b Â ⁻ \$\$ boverline{b} \$\$ produced in association with top quarks decaying hadronically in pp collisions at s = 8 \$\$ sqrt{s}=8 \$\$ TeV with the ATLAS detector. Journal of High Energy Physics, 2016, 2016, 1.	4.7	21
260	Search for Higgs boson pair production in the WW(*)WW(*) decay channel using ATLAS data recorded at \$\$ sqrt{mathrm{s}} \$\$ = 13 TeV. Journal of High Energy Physics, 2019, 2019, 1.	4.7	21
261	Identification of boosted Higgs bosons decaying into b-quark pairs with the ATLAS detector at 13Â\$\$ext {TeV}\$\$. European Physical Journal C, 2019, 79, .	3.9	21
262	Search for light long-lived neutral particles produced in pp collisions at \$\$sqrt{s} = 13~mathrm {TeV}\$\$ and decaying into collimated leptons or light hadrons with the ATLAS detector. European Physical Journal C, 2020, 80, 1.	3.9	21
263	Benefit and toxicity of programmed death-1 blockade vary by ethnicity in patients with advanced melanoma: an international multicentre observational study. British Journal of Dermatology, 2022, 187, 401-410.	1.5	21
264	Search for new phenomena in events with a photon and missing transverse momentum in pp collisions at s = 13 \$\$ sqrt{s}=13 \$\$ TeV with the ATLAS detector. Journal of High Energy Physics, 2016, 2016, 1.	4.7	20
265	Measurements of top quark spin observables in t t Â ⁻ \$\$ toverline{t} \$\$ events using dilepton final states in s = 8 \$\$ sqrt{s}=8 \$\$ TeV pp collisions with the ATLAS detector. Journal of High Energy Physics, 2017, 2017, 1.	4.7	20
266	Measurement of differential cross-sections of a single top quark produced in association with a W boson at \$\$sqrt{s}={13}{ext {TeV}}\$\$ s = 13 TeV with ATLAS. European Physical Journal C, 2018, 78, 186.	3.9	20
267	Frequent genetic aberrations in the cell cycle related genes in mucosal melanoma indicate the potential for targeted therapy. Journal of Translational Medicine, 2019, 17, 245.	4.4	20
268	Search for diboson resonances in hadronic final states in 139 fbâ^'1 of pp collisions at \$\$ sqrt{s} \$\$ = 13 TeV with the ATLAS detector. Journal of High Energy Physics, 2019, 2019, 1.	4.7	20
269	Measurement of k T splitting scales in W→ℓν events at \$sqrt{s} = 7 mathrm{TeV}\$ with the ATLAS detector. European Physical Journal C, 2013, 73, 2432.	3.9	19
270	Search for flavour-changing neutral current top quark decays t → Hq in pp collisions at s = 8 \$\$ sqrt{s}=8 \$\$ TeV with the ATLAS detector. Journal of High Energy Physics, 2015, 2015, 1-65.	4.7	19

#	Article	IF	CITATIONS
271	Search for the production of single vector-like and excited quarks in the Wt final state in pp collisions at s = 8 \$\$ sqrt{s}=8 \$\$ TeV with the ATLAS detector. Journal of High Energy Physics, 2016, 2016, 1.	4.7	19
272	Probing lepton flavour violation via neutrinoless \$\$varvec{au longrightarrow 3mu }\$\$ Ï,, ⟶ 3 μ decays with the ATLAS detector. European Physical Journal C, 2016, 76, 232.	3.9	19
273	Measurement of detector-corrected observables sensitive to the anomalous production of events with jets and large missing transverse momentum in \$\$varvec{pp}\$\$ p p collisions at \$\$mathbf {sqrt{s}=13}\$\$ s = 13 ÂTeV using the ATLAS detector. European Physical Journal C, 2017, 77, 765.	3.9	19
274	Analysis of NRAS gain in 657 patients with melanoma and evaluation of its sensitivity to a MEK inhibitor. European Journal of Cancer, 2018, 89, 90-101.	2.8	19
275	Prompt and non-prompt \$\$J/psi \$\$ J / ï^ elliptic flow in Pb+Pb collisions at \$\$sqrt{s_{_ext {NN}}} = 5.02\$\$ s NN = 5.02 Tev with the ATLAS detectorÂ. European Physical Journal C, 2018, 78, 784.	3.9	19
276	High G2 and Sâ€phase expressed 1 expression promotes acral melanoma progression and correlates with poor clinical prognosis. Cancer Science, 2018, 109, 1787-1798.	3.9	19
277	Search for top-quark decays t → Hq with 36 fbâ^'1 of pp collision data at \$\$ sqrt{s} \$\$ = 13 TeV with the ATLAS detector. Journal of High Energy Physics, 2019, 2019, 1.	4.7	19
278	Characterization and adsorption of a Lactobacillus plantarum virulent phage. Journal of Dairy Science, 2019, 102, 3879-3886.	3.4	19
279	Search for squarks and gluinos in final states with same-sign leptons and jets using 139 fbâ^'1 of data collected with the ATLAS detector. Journal of High Energy Physics, 2020, 2020, 1.	4.7	19
280	Measurement of light-by-light scattering and search for axion-like particles with 2.2 nbâ^'1 of Pb+Pb data with the ATLAS detector. Journal of High Energy Physics, 2021, 2021, 1.	4.7	19
281	Palbociclib in advanced acral melanoma with genetic aberrations in the cyclin-dependent kinase 4 pathway. European Journal of Cancer, 2021, 148, 297-306.	2.8	19
282	Search for top quark decays t → qH, with H → γγ, in s = 13 \$\$ sqrt{s}=13 \$\$ TeV pp collisions using the ATLAS detector. Journal of High Energy Physics, 2017, 2017, 1.	4.7	18
283	Search for dark matter in association with an energetic photon in pp collisions at \$\$ sqrt{s} \$\$ = 13 TeV with the ATLAS detector. Journal of High Energy Physics, 2021, 2021, 1.	4.7	18
284	Search for pair production of scalar leptoquarks decaying into first- or second-generation leptons and top quarks in proton–proton collisions at \$\$sqrt{s}\$\$ = 13ÂTeV with the ATLAS detector. European Physical Journal C, 2021, 81, 1.	3.9	18
285	Search for new phenomena in final states with b-jets and missing transverse momentum in \$\$ sqrt{mathrm{s}} \$\$ = 13 TeV pp collisions with the ATLAS detector. Journal of High Energy Physics, 2021, 2021, 1.	4.7	18
286	Identification of high transverse momentum top quarks in pp collisions at s = 8 \$\$ sqrt{s}=8 \$\$ TeV with the ATLAS detector. Journal of High Energy Physics, 2016, 2016, 1.	4.7	17
287	Probing the W tb vertex structure in t-channel single-top-quark production and decay in pp collisions at s = 8 \$\$ sqrt{s}=8 \$\$ TeV with the ATLAS detector. Journal of High Energy Physics, 2017, 2017, 1.	4.7	17
288	Search for supersymmetry in events with b-tagged jets and missing transverse momentum in pp collisions at \$\$ sqrt{s}=13 \$\$ TeV with the ATLAS detector. Journal of High Energy Physics, 2017, 2017, 1.	4.7	17

#	Article	IF	CITATIONS
289	Measurement of the cross-section for producing a W boson in association with a single top quark in pp collisions at s = 13 \$\$ sqrt{s}=13 \$\$ TeV with ATLAS. Journal of High Energy Physics, 2018, 2018, 1.	4.7	17
290	Direct top-quark decay width measurement in the \$\$mathbf {varvec{tar{t}}}\$\$ t t Â ⁻ lepton+jets channel at \$\$sqrt{s}=8~ext {TeV}\$\$ s = 8 TeV with the ATLAS experiment. European Physical Journal C, 2018, 78, 129.	3.9	17
291	Search for flavour-changing neutral current top-quark decays t → qZ in proton-proton collisions at \$\$ sqrt{s}=13 \$\$ TeV with the ATLAS detector. Journal of High Energy Physics, 2018, 2018, 1.	4.7	17
292	Measurement of inclusive jet and dijet cross-sections in proton-proton collisions at \$\$ sqrt{s}=13 \$\$ TeV with the ATLAS detector. Journal of High Energy Physics, 2018, 2018, 1.	4.7	17
293	Measurements of W and Z boson production in pp collisions at \$\$sqrt{s}=5.02\$\$ s = 5.02 ÂTeV with the ATLAS detector. European Physical Journal C, 2019, 79, 1.	3.9	17
294	Measurement of \$\$W^pm \$\$ boson production in Pb+Pb collisions at \$\$sqrt{s_{mathrm{NN}}} = 5.02~ext {Te}ext {V}\$\$ with the ATLAS detector. European Physical Journal C, 2019, 79, 1.	3.9	17
295	Performance of the missing transverse momentum triggers for the ATLAS detector during Run-2 data taking. Journal of High Energy Physics, 2020, 2020, 1.	4.7	17
296	Search for the HH → \$\$ boverline{b}boverline{b} \$\$ process via vector-boson fusion production using proton-proton collisions at \$\$ sqrt{s} \$\$ = 13 TeV with the ATLAS detector. Journal of High Energy Physics, 2020, 2020, 1.	4.7	17
297	Search for type-III seesaw heavy leptons in dilepton final states in pp collisions at \$\$ sqrt{s} = 13,{ext {TeV}} \$\$ with the ATLAS detector. European Physical Journal C, 2021, 81, 1.	3.9	17
298	Dark matter interpretations of ATLAS searches for the electroweak production of supersymmetric particles in s = 8 \$\$ sqrt{s}=8 \$\$ TeV proton-proton collisions. Journal of High Energy Physics, 2016, 2016, 1.	4.7	16
299	Measurements of top-quark pair differential cross-sections in the lepton+jets channel in pp collisions at \$\$ sqrt{s}=13 \$\$ TeV using the ATLAS detector. Journal of High Energy Physics, 2017, 2017, 1.	4.7	16
300	Top-quark mass measurement in the all-hadronic t t \hat{A}^- \$\$ toverline{t} \$\$ decay channel at s = 8 \$\$ sqrt{s}=8 \$\$ TeV with the ATLAS detector. Journal of High Energy Physics, 2017, 2017, 1.	4.7	16
301	Measurement of colour flow using jet-pull observables in \$\$tar{t}\$\$ t t Â⁻ events with the ATLAS experiment at \$\$sqrt{s} = 13,hbox {TeV}\$\$ s = 13 TeV. European Physical Journal C, 2018, 78, 847.	3.9	16
302	Search for exclusive Higgs and Z boson decays to ï•γ and ïŀ³ with the ATLAS detector. Journal of High Energy Physics, 2018, 2018, 1.	4.7	16
303	Measurement of differential cross sections and W+/Wâ^' cross-section ratios for W boson production in association with jets at \$\$ sqrt{s}=8 \$\$ TeV with the ATLAS detector. Journal of High Energy Physics, 2018, 2018, 1.	4.7	16
304	An open-label, single-arm, multicenter, phase II study of RC48-ADC to evaluate the efficacy and safety of subjects with HER2 overexpressing locally advanced or metastatic urothelial cancer (RC48-C009) Journal of Clinical Oncology, 2021, 39, 4584-4584.	1.6	16
305	Palbociclib for treatment of metastatic melanoma with copy number variations of CDK4 pathway: case report. Chinese Clinical Oncology, 2018, 7, 62-62.	1.2	16
306	Treatment algorithm of metastatic mucosal melanoma. Chinese Clinical Oncology, 2014, 3, 38.	1.2	16

#	Article	IF	CITATIONS
307	Measurement of event-shape observables in \$\$Z ightarrow ell ^{+} ell ^{-}\$\$ Z → ℓ + ℓ - events in pp collisions at \$\$sqrt{s}=7\$\$ s = 7 Â \$\${mathrm{TeV}}\$\$ TeV with the ATLAS detector at the LHC. European Physical Journal C, 2016, 76, 375.	3.9	15
308	Measurement of fiducial differential cross sections of gluon-fusion production of Higgs bosons decaying to WW â^—→eνμν with the ATLAS detector at s = 8 \$\$ sqrt{s}=8 \$\$ TeV. Journal of High Energy Physics, 2016, 2016, 1.	4.7	15
309	Search for strong gravity in multijet final states produced in pp collisions at s = 13 \$\$ sqrt{s}=13 \$\$ TeV using the ATLAS detector at the LHC. Journal of High Energy Physics, 2016, 2016, 1.	4.7	15
310	Search for supersymmetry in final states with charm jets and missing transverse momentum in 13 TeV pp collisions with the ATLAS detector. Journal of High Energy Physics, 2018, 2018, 1.	4.7	15
311	Search for scalar resonances decaying into μ+μâ^' in events with and without b-tagged jets produced in proton-proton collisions at \$\$ sqrt{s}=13 \$\$ TeV with the ATLAS detector. Journal of High Energy Physics, 2019, 2019, 1.	4.7	15
312	The Impact of Liver Metastasis on Anti-PD-1 Monoclonal Antibody Monotherapy in Advanced Melanoma: Analysis of Five Clinical Studies. Frontiers in Oncology, 2020, 10, 546604.	2.8	15
313	Toripalimab for the treatment of melanoma. Expert Opinion on Biological Therapy, 2020, 20, 863-869.	3.1	15
314	Optimisation of large-radius jet reconstruction for the ATLAS detector in 13ÂTeV proton–proton collisions. European Physical Journal C, 2021, 81, 1.	3.9	15
315	The <i>TERT</i> copy number gain is sensitive to telomerase inhibitors in human melanoma. Clinical Science, 2020, 134, 193-205.	4.3	15
316	Determination of jet calibration and energy resolution in proton–proton collisions at \$\$sqrt{s} = 8~hbox {TeV}\$\$ using the ATLAS detector. European Physical Journal C, 2020, 80, 1.	3.9	15
317	An Evidence-Based Staging System for Mucosal Melanoma: A Proposal. Annals of Surgical Oncology, 2022, 29, 5221-5234.	1.5	15
318	A phase II study of RC48-ADC in HER2-negative patients with locally advanced or metastatic urothelial carcinoma Journal of Clinical Oncology, 2022, 40, 4519-4519.	1.6	15
319	A search for top squarks with R-parity-violating decays to all-hadronic final states with the ATLAS detector in s = 8 \$\$ sqrt{s}=8 \$\$ TeV proton-proton collisions. Journal of High Energy Physics, 2016, 2016, 1.	4.7	14
320	Measurement of the production cross-section of a single top quark in association with a W boson at 8 TeV with the ATLAS experiment. Journal of High Energy Physics, 2016, 2016, 1.	4.7	14
321	Measurement of charged-particle distributions sensitive to the underlying event in s = 13 \$\$ sqrt{s}=13 \$\$ TeV proton-proton collisions with the ATLAS detector at the LHC. Journal of High Energy Physics, 2017, 2017, 1.	4.7	14
322	Studies of ZÎ ³ production in association with a high-mass dijet system in pp collisions at s = 8 \$\$ sqrt{s}=8 \$\$ TeV with the ATLAS detector. Journal of High Energy Physics, 2017, 2017, 1.	4.7	14
323	Measurement of VH, \$\$ mathrm{H}o mathrm{b}overline{mathrm{b}} \$\$ production as a function of the vector-boson transverse momentum in 13 TeV pp collisions with the ATLAS detector. Journal of High Energy Physics, 2019, 2019, 1.	4.7	14
324	Measurements of inclusive and differential fiducial cross-sections of \$\$tar{t}gamma \$\$ production in leptonic final states at \$\$sqrt{s}=13~ext {TeV}\$\$ in ATLAS. European Physical Journal C, 2019, 79, 1.	3.9	14

#	Article	IF	CITATIONS
325	Search for bottom-squark pair production with the ATLAS detector in final states containing Higgs bosons, b-jets and missing transverse momentum. Journal of High Energy Physics, 2019, 2019, 1.	4.7	14
326	Search for new phenomena with top quark pairs in final states with one lepton, jets, and missing transverse momentum in pp collisions at \$\$ sqrt{s} \$\$ = 13 TeV with the ATLAS detector. Journal of High Energy Physics, 2021, 2021, 1.	4.7	14
327	Measurements of Higgs bosons decaying to bottom quarks from vector boson fusion production with the ATLAS experiment at \$\$sqrt{s}=13,ext {TeV}\$\$. European Physical Journal C, 2021, 81, 1.	3.9	14
328	EZH2 Inhibitor Enhances the STING Agonist‒Induced Antitumor Immunity in Melanoma. Journal of Investigative Dermatology, 2022, 142, 1158-1170.e8.	0.7	14
329	Measurements of top-quark pair single- and double-differential cross-sections in the all-hadronic channel in pp collisions at \$\$ sqrt{mathrm{s}} \$\$ = 13 TeV using the ATLAS detector. Journal of High Energy Physics, 2021, 2021, 1.	4.7	14
330	Search for \$\$ toverline{t} \$\$ resonances in fully hadronic final states in pp collisions at \$\$ sqrt{s} \$\$ = 13 TeV with the ATLAS detector. Journal of High Energy Physics, 2020, 2020, 1.	4.7	14
331	Genotyping of mucosal melanoma. Chinese Clinical Oncology, 2014, 3, 34.	1.2	14
332	Measurement of the c-jet mistagging efficiency in \$\$tar{t}\$\$Âevents using pp collision data at \$\$sqrt{s}=13\$\$Â\$\$ext {TeV}\$\$ collected with the ATLAS detector. European Physical Journal C, 2022, 82, .	3.9	14
333	Human skin neural crest progenitor cells are susceptible to BRAFV600E-induced transformation. Oncogene, 2014, 33, 832-841.	5.9	13
334	Measurement of the CP-violating phase ï• s and the B s 0 meson decay width difference with B s 0  → J/ľ decays in ATLAS. Journal of High Energy Physics, 2016, 2016, 1.	Ï∙ 4.7	13
335	Search for new phenomena with photon+jet events in proton-proton collisions at s = 13 \$\$ sqrt{s}=13 \$\$ TeV with the ATLAS detector. Journal of High Energy Physics, 2016, 2016, 1.	4.7	13
336	Search for anomalous couplings in the W tb vertex from the measurement of double differential angular decay rates of single top quarks produced in the t-channel with the ATLAS detector. Journal of High Energy Physics, 2016, 2016, 1-46.	4.7	13
337	Measurements of top-quark pair to Z-boson cross-section ratios at s = 13 \$\$ sqrt{s}=13 \$\$, 8, 7 TeV with the ATLAS detector. Journal of High Energy Physics, 2017, 2017, 1.	4.7	13
338	Search for new phenomena in high-mass final states with a photon and a jet from \$\$pp\$\$ pp collisions at \$\$sqrt{s}\$\$ s. European Physical Journal C, 2018, 78, 102.	3.9	13
339	Identification of a functional polymorphism within the 3′-untranslated region of denticleless E3 ubiquitin protein ligase homolog associated with survival in acral melanoma. European Journal of Cancer, 2019, 118, 70-81.	2.8	13
340	Measurement of jet-substructure observables in top quark, W boson and light jet production in proton-proton collisions at \$\$ sqrt{s} \$\$ = 13 TeV with the ATLAS detector. Journal of High Energy Physics, 2019, 2019, 1.	4.7	13
341	Search for squarks and gluinos in final states with one isolated lepton, jets, and missing transverse momentum at \$\$sqrt{s}=13\$\$ TeV with the ATLAS detector. European Physical Journal C, 2021, 81, 1.	3.9	13
342	OrienX010, an oncolytic virus, in patients with unresectable stage IIIC–IV melanoma: a phase Ib study. ,		13

342 2022, 10, e004307.

#	Article	IF	CITATIONS
343	Measurement of the \$\$boverline{b}\$\$ b b Â ⁻ dijet cross section in pp collisions at \$\$sqrt{s} = 7\$\$ s = 7 ÂTeV with the ATLAS detector. European Physical Journal C, 2016, 76, 670.	3.9	12
344	Search for new phenomena in events containing a same-flavour opposite-sign dilepton pair, jets, and large missing transverse momentum in \$\$varvec{sqrt{s}=13}\$\$ s = 13 Â \$\$ext {TeV}\$\$ TeV \$\$varvec{pp}\$\$ p p collisions with the ATLAS detector. European Physical Journal C, 2017, 77, 144.	3.9	12
345	Search for new phenomena in a lepton plus high jet multiplicity final state with the ATLAS experiment using s = 13 \$\$ sqrt{s}=13 \$\$ TeV proton-proton collision data. Journal of High Energy Physics, 2017, 2017, 1.	4.7	12
346	Unconventional myosin VIIA promotes melanoma progression. Journal of Cell Science, 2018, 131, .	2.0	12
347	Analysis of TSC1 mutation spectrum in mucosal melanoma. Journal of Cancer Research and Clinical Oncology, 2018, 144, 257-267.	2.5	12
348	Observation of the associated production of a top quark and a Z boson in pp collisions at \$\$ sqrt{s} \$\$= 13 TeV with the ATLAS detector. Journal of High Energy Physics, 2020, 2020, 1.	4.7	12
349	Search for new phenomena in final states with large jet multiplicities and missing transverse momentum using \$\$ sqrt{s} \$\$ = 13 TeV proton-proton collisions recorded by ATLAS in Run 2 of the LHC. Journal of High Energy Physics, 2020, 2020, 1.	4.7	12
350	Pazopanib versus sunitinib in Chinese patients with locally advanced or metastatic renal cell carcinoma: pooled subgroup analysis from the randomized, COMPARZ studies. BMC Cancer, 2020, 20, 219.	2.6	12
351	Phase 1 trial of vorolanib (CM082) in combination with everolimus in patients with advanced clear-cell renal cell carcinoma. EBioMedicine, 2020, 55, 102755.	6.1	12
352	Transverse momentum and process dependent azimuthal anisotropies in \$\$sqrt{s_{mathrm {NN}}=8.16\$\$ÂTeV p+Pb collisions with the ATLAS detector. European Physical Journal C, 2020, 80, 1.	3.9	12
353	Differential cross-section measurements for the electroweak production of dijets in association with a Z boson in proton–proton collisions at ATLAS. European Physical Journal C, 2021, 81, 1.	3.9	12
354	Search for supersymmetry in events with four or more charged leptons in 139 fbâ^'1 of \$\$ sqrt{s} \$\$ = 13 TeV pp collisions with the ATLAS detector. Journal of High Energy Physics, 2021, 2021, 1.	4.7	12
355	Measurements of the inclusive and differential production cross sections of a top-quark–antiquark pair in association with a ZÂboson at \$\$sqrt{s} = 13\$\$ÂTeV with the ATLAS detector. European Physical Journal C, 2021, 81, 1.	3.9	12
356	Search for dark matter in events with missing transverse momentum and a Higgs boson decaying into two photons in pp collisions at \$\$ sqrt{s} \$\$ = 13 TeV with the ATLAS detector. Journal of High Energy Physics, 2021, 2021, 1.	4.7	12
357	Alignment of the ATLAS Inner Detector in Run 2. European Physical Journal C, 2020, 80, 1.	3.9	12
358	Determination of the parton distribution functions of the proton using diverse ATLAS data from pp collisions at \$\$sqrt{s} = 7\$\$, 8 and 13ÂTeV. European Physical Journal C, 2022, 82, 1.	3.9	12
359	Preliminary results of a phase Ib/II combination study of RC48-ADC, a novel humanized anti-HER2 antibody-drug conjugate (ADC) with toripalimab, a humanized IgG4 mAb against programmed death-1 (PD-1) in patients with locally advanced or metastatic urothelial carcinoma Journal of Clinical Oncology, 2022, 40, 4518-4518.	1.6	12
360	Simplified supersymmetry with sneutrino LSP at 8 TeV LHC. Journal of High Energy Physics, 2014, 2014, 1.	4.7	11

#	Article	IF	CITATIONS
361	Measurement of four-jet differential cross sections in s = 8 \$\$ sqrt{s}=8 \$\$ TeV proton-proton collisions using the ATLAS detector. Journal of High Energy Physics, 2015, 2015, 1-76.	4.7	11
362	Beam-induced and cosmic-ray backgrounds observed in the ATLAS detector during the LHC 2012 proton-proton running period. Journal of Instrumentation, 2016, 11, P05013-P05013.	1.2	11
363	Search for squarks and gluinos in events with hadronically decaying tau leptons, jets and missing transverse momentum in proton–proton collisions at \$\$sqrt{s}=13\$\$ s = 13 ATeV recorded with the ATLAS detector. European Physical Journal C, 2016, 76, 683.	3.9	11
364	Measurement of jet activity produced in top-quark events with an electron, a muon and two b-tagged jets in the final state in pp collisions at \$\$sqrt{s}=13\$\$ s = 13 TeV with the ATLAS detector. European Physical Journal C, 2017, 77, 220.	3.9	11
365	Search for new phenomena with large jet multiplicities and missing transverse momentum using large-radius jets and flavour-tagging at ATLAS in 13 TeV pp collisions. Journal of High Energy Physics, 2017, 2017, 1.	4.7	11
366	Measurements of the production cross-section for a Z boson in association with b-jets in proton-proton collisions at \$\$ sqrt{s} \$\$ = 13 TeV with the ATLAS detector. Journal of High Energy Physics, 2020, 2020, 1.	4.7	11
367	Chemotherapy, biochemotherapy and anti-VEGF therapy in metastatic mucosal melanoma. Chinese Clinical Oncology, 2014, 3, 36.	1.2	11
368	Search for direct top squark pair production in final states with two tau leptons in pp collisions at \$\$sqrt{s}=8\$\$ s = 8 ÂTeV with the ATLAS detector. European Physical Journal C, 2016, 76, 81.	3.9	10
369	Nanosecond Pulsed Electric Fields Enhance the Anti-tumour Effects of the mTOR Inhibitor Everolimus against Melanoma. Scientific Reports, 2017, 7, 39597.	3.3	10
370	Gene expression screening identifies CDCA5 as a potential therapeutic target in acral melanoma. Human Pathology, 2018, 75, 137-145.	2.0	10
371	Measurement of the \$\$ Zgamma o u overline{u}gamma \$\$ production cross section in pp collisions at \$\$ sqrt{s}=13 \$\$ TeV with the ATLAS detector and limits on anomalous triple gauge-boson couplings. Journal of High Energy Physics, 2018, 2018, 1.	4.7	10
372	Measurement of the inclusive and fiducial $ftar{t}\$ t t \hat{A}^{-} production cross-sections in the. European Physical Journal C, 2018, 78, 487.	3.9	10
373	Vemurafenib in Chinese patients with BRAFV600 mutation–positive unresectable or metastatic melanoma: an open-label, multicenter phase I study. BMC Cancer, 2018, 18, 520.	2.6	10
374	First-line axitinib versus sorafenib in Asian patients with metastatic renal cell carcinoma: exploratory subgroup analyses of Phase III data. Future Oncology, 2019, 15, 53-63.	2.4	10
375	Determination of the parton distribution functions of the proton from ATLAS measurements of differential W± and Z boson production in association with jets. Journal of High Energy Physics, 2021, 2021, 1.	4.7	10
376	Association of NRAS Mutation With Clinical Outcomes of Anti-PD-1 Monotherapy in Advanced Melanoma: A Pooled Analysis of Four Asian Clinical Trials. Frontiers in Immunology, 2021, 12, 691032.	4.8	10
377	Measurement of J/̈́ production in association with a W± boson with pp data at 8 TeV. Journal of High Energy Physics, 2020, 2020, 1.	4.7	10
378	Measurement of the t\$\$ overline{t} \$\$t\$\$ overline{t} \$\$ production cross section in pp collisions at \$\$ sqrt{s} \$\$ = 13 TeV with the ATLAS detector. Journal of High Energy Physics, 2021, 2021, 1.	4.7	10

#	Article	IF	CITATIONS
379	Search for Higgs bosons decaying into new spin-0 or spin-1 particles in four-lepton final states with the ATLAS detector with 139 fbâ 1 of pp collision data at \$\$ sqrt{s} \$\$ = 13 TeV. Journal of High Energy Physics, 2022, 2022, 1.	4.7	10
380	Search for dark matter produced in association with a Standard Model Higgs boson decaying into b-quarks using the full Run 2 dataset from the ATLAS detector. Journal of High Energy Physics, 2021, 2021, 1.	4.7	10
381	A new method to distinguish hadronically decaying boosted Z bosons from W bosons using the ATLAS detector. European Physical Journal C, 2016, 76, 238.	3.9	9
382	Measurement of the \$\$ toverline{t}gamma \$\$ production cross section in proton-proton collisions at \$\$ sqrt{s}=8 \$\$ TeV with the ATLAS detector. Journal of High Energy Physics, 2017, 2017, 1.	4.7	9
383	Measurements of charge and CP asymmetries in b-hadron decays using top-quark events collected by the ATLAS detector in pp collisions at s = 8 \$\$ sqrt{s}=8 \$\$ TeV. Journal of High Energy Physics, 2017, 2017, 1.	4.7	9
384	Measurement of the ZZ production cross section in proton-proton collisions at s = 8 \$\$ sqrt{s}=8 \$\$ TeV using the ZZ → â""â"â""+ℓ′â"ℓ′+ and Z Z → â"" â" â"" + ν ν Â⁻ \$\$ ZZo {ell}^{-}{ell}^{+}u ove with the ATLAS detector. Journal of High Energy Physics, 2017, 2017, 1.	rli m.e {u}\$	\$ d ecay char
385	Measurements of differential cross sections of top quark pair production in association with jets in pp collisions at \$\$ sqrt{s}=13 \$\$ TeV using the ATLAS detector. Journal of High Energy Physics, 2018, 2018, 1.	4.7	9
386	Measurement of the inclusive cross-section for the production of jets in association with a Z boson in proton–proton collisions at 8ÂTeV using the ATLAS detector. European Physical Journal C, 2019, 79, 1.	3.9	9
387	Measurement of the Z(→ â,,"+â,,"â^')γ production cross-section in pp collisions at \$\$ sqrt{s} \$\$ = 13 TeV with th ATLAS detector. Journal of High Energy Physics, 2020, 2020, 1.	າe 4.7	9
388	Clinicopathological characteristics, prognosis, and chemosensitivity in patients with metastatic upper tract urothelial carcinoma. Urologic Oncology: Seminars and Original Investigations, 2021, 39, 75.e1-75.e8.	1.6	9
389	A phase 2 clinical trial of neoadjuvant anti-PD-1 ab (Toripalimab) plus axitinib in resectable mucosal melanoma Journal of Clinical Oncology, 2021, 39, 9512-9512.	1.6	9
390	Overall Survival of Patients With Unresectable or Metastatic BRAF V600-Mutant Acral/Cutaneous Melanoma Administered Dabrafenib Plus Trametinib: Long-Term Follow-Up of a Multicenter, Single-Arm Phase IIa Trial. Frontiers in Oncology, 2021, 11, 720044.	2.8	9
391	Search for dark matter produced in association with a single top quark in \$\$sqrt{s}=13\$\$ÂTeV \$\$pp\$\$ collisions with the ATLAS detector. European Physical Journal C, 2021, 81, 1.	3.9	9
392	Prognostic value of ulceration varies across Breslow thicknesses and clinical stages in acral melanoma: a retrospective study*. British Journal of Dermatology, 2022, 186, 977-987.	1.5	9
393	Measurement of the relative width difference of the B 0 ―B Â⁻ 0 \$\$ {B}^Ohbox{-} {overline{B}}^0 \$\$ system with the ATLAS detector. Journal of High Energy Physics, 2016, 2016, 1.	4.7	8
394	Search for direct top squark pair production in events with a Higgs or Z boson, and missing transverse momentum in s = 13 \$\$ sqrt{s}=13 \$\$ TeV pp collisions with the ATLAS detector. Journal of High Energy Physics, 2017, 2017, 1.	4.7	8
395	Measurement of b-hadron pair production with the ATLAS detector in proton-proton collisions at \$\$ sqrt{s}=8 \$\$ TeV. Journal of High Energy Physics, 2017, 2017, 1.	4.7	8
396	Analysis of the Wtb vertex from the measurement of triple-differential angular decay rates of single top quarks produced in the t-channel at s = 8 \$\$ sqrt{s}=8 \$\$ TeV with the ATLAS detector. Journal of High Energy Physics, 2017, 2017, 1.	4.7	8

#	Article	IF	CITATIONS
397	Safety and Efficacy of Apatinib Combined with Temozolomide in Advanced Melanoma Patients after Conventional Treatment Failure. Translational Oncology, 2018, 11, 1155-1159.	3.7	8
398	Search for large missing transverse momentum in association with one top-quark in proton-proton collisions at \$\$ sqrt{s} \$\$ = 13 TeV with the ATLAS detector. Journal of High Energy Physics, 2019, 2019, 1.	4.7	8
399	Potential Mutations in Uveal Melanoma Identified Using Targeted Next-Generation Sequencing. Journal of Cancer, 2019, 10, 488-493.	2.5	8
400	Measurement of \$\$W^{pm }\$\$-boson and Z-boson production cross-sections in pp collisions at \$\$sqrt{s}=2.76\$\$ÂTeV with the ATLAS detector. European Physical Journal C, 2019, 79, 1.	3.9	8
401	Measurement of differential cross sections for single diffractive dissociation in \$\$ sqrt{s} \$\$ = 8 TeV pp collisions using the ATLAS ALFA spectrometer. Journal of High Energy Physics, 2020, 2020, 1.	4.7	8
402	A Functional Synonymous Variant in <i>PDGFRA</i> Is Associated with Better Survival in Acral Melanoma. Journal of Cancer, 2020, 11, 2945-2956.	2.5	8
403	Measurements of W+Wâ^+ ≥ 1 jet production cross-sections in pp collisions at \$\$ sqrt{s} \$\$ = 13 TeV with the ATLAS detector. Journal of High Energy Physics, 2021, 2021, 1.	4.7	8
404	Measurements of differential cross-sections in four-lepton events in 13 TeV proton-proton collisions with the ATLAS detector. Journal of High Energy Physics, 2021, 2021, 1.	4.7	8
405	Reconstruction and identification of boosted di-ï,, systems in a search for Higgs boson pairs using 13 TeV proton-proton collision data in ATLAS. Journal of High Energy Physics, 2020, 2020, 1.	4.7	8
406	Observation of electroweak production of two jets in association with an isolated photon and missing transverse momentum, and search for a Higgs boson decaying into invisible particles at 13Â\$\$ext {TeV}\$\$ with the ATLAS detector. European Physical Journal C, 2022, 82, 1.	3.9	8
407	Does MYC2 really play a negative role in jasmonic acid-induced indolic glucosinolate biosynthesis in Arabidopsis thaliana?. Russian Journal of Plant Physiology, 2013, 60, 100-107.	1.1	7
408	Outcomes and Predictive Factors of Isolated Limb Infusion for Patients with In-transit Melanoma in China. Annals of Surgical Oncology, 2018, 25, 885-893.	1.5	7
409	Increased <i>AURKA</i> Gene Copy Number Correlates with Poor Prognosis and Predicts the Efficacy of High-dose Interferon Therapy in Acral Melanoma. Journal of Cancer, 2018, 9, 1267-1276.	2.5	7
410	Measurement of \$\$au \$\$ Ï,, polarisation in \$\$Z/gamma ^{*}ightarrow au au \$\$ Z / γ. European Physical Journal C, 2018, 78, 163.	3.9	7
411	MUC4 isoforms expression profiling and prognosis value in Chinese melanoma patients. Clinical and Experimental Medicine, 2020, 20, 299-311.	3.6	7
412	Search for dijet resonances in events with an isolated charged lepton using \$\$ sqrt{s} \$\$ = 13 TeV proton-proton collision data collected by the ATLAS detector. Journal of High Energy Physics, 2020, 2020, 1.	4.7	7
413	The combination therapy with the cytotoxic T lymphocyte-associated antigen-4 and programmed death 1 antibody-induced asthma in a patient with advanced melanoma. Journal of Cancer Research and Therapeutics, 2021, 17, 808.	0.9	7
414	Radiological dynamics and SITC-defined resistance types of advanced melanoma during anti-PD-1 monotherapy: an independent single-blind observational study on an international cohort. , 2021, 9, e002092.		7

#	Article	IF	CITATIONS
415	Real-world efficacy and safety of axitinib in combination with anti-programmed cell death-1 antibody for advanced mucosal melanoma. European Journal of Cancer, 2021, 156, 83-92.	2.8	7
416	Search for R-parity-violating supersymmetry in a final state containing leptons and many jets with the ATLAS experiment using \$\$sqrt{s} = 13hbox { TeV}\$\$ proton–proton collision data. European Physical Journal C, 2021, 81, 1.	3.9	7
417	Configuration and performance of the ATLAS b-jet triggers in Run 2. European Physical Journal C, 2021, 81, 1.	3.9	7
418	Search for flavour-changing neutral-current interactions of a top quark and a gluon in pp collisions at \$\$sqrt{s}=13\$\$ÂTeV with the ATLAS detector. European Physical Journal C, 2022, 82, .	3.9	7
419	Evolving Treatment Approaches to Mucosal Melanoma. Current Oncology Reports, 2022, 24, 1261-1271.	4.0	7
420	Measurement of the ratio of cross sections for inclusive isolated-photon production in pp collisions at \$\$ sqrt{s} \$\$ = 13 and 8 TeV with the ATLAS detector. Journal of High Energy Physics, 2019, 2019, 1.	4.7	6
421	Measurement of ZZ production in the ℓℓνν final state with the ATLAS detector in pp collisions at \$\$ sqrt{s} \$\$ = 13 TeV. Journal of High Energy Physics, 2019, 2019, 1.	4.7	6
422	Chemotherapy combined with antiangiogenic drugs as salvage therapy in advanced melanoma patients progressing on PD-1 immunotherapy. Translational Oncology, 2021, 14, 100949.	3.7	6
423	Search for Higgs boson production in association with a high-energy photon via vector-boson fusion with decay into bottom quark pairs at \$\$ sqrt{s} \$\$ = 13 TeV with the ATLAS detector. Journal of High Energy Physics, 2021, 2021, 1.	4.7	6
424	Risk Models for Advanced Melanoma Patients Under Anti-PD-1 Monotherapy—Ad hoc Analyses of Pooled Data From Two Clinical Trials. Frontiers in Oncology, 2021, 11, 639085.	2.8	6
425	Performance of the ATLAS Level-1 topological trigger in RunÂ2. European Physical Journal C, 2022, 82, 1.	3.9	6
426	The Phase-I trigger readout electronics upgrade of the ATLAS Liquid Argon calorimeters. Journal of Instrumentation, 2022, 17, P05024.	1.2	6
427	Measurement of long-range two-particle azimuthal correlations in Z-boson tagged pp collisions at \$\$sqrt{s}=8\$\$ and 13ÂTeV. European Physical Journal C, 2020, 80, 1.	3.9	5
428	Realâ€ŧime monitoring of single circulating tumor cells with a fluorescently labeled deoxyâ€glucose by in vivo flow cytometry. Cytometry Part A: the Journal of the International Society for Analytical Cytology, 2021, 99, 586-592.	1.5	5
429	A phase Ib clinical trial of neoadjuvant OrienX010, an oncolytic virus, in combination with toripalimab in patients with resectable stage IIIb to stage IVM1a acral melanoma Journal of Clinical Oncology, 2021, 39, 9570-9570.	1.6	5
430	Atezolizumab in combination with bevacizumab in patients with unresectable locally advanced or metastatic mucosal melanoma: Interim analysis of an open-label phase II trial Journal of Clinical Oncology, 2021, 39, 9511-9511.	1.6	5
431	A search for the decays of stopped long-lived particles at \$\$ sqrt{mathrm{s}} \$\$ = 13 TeV with the ATLAS detector. Journal of High Energy Physics, 2021, 2021, 1.	4.7	5
432	Search for phenomena beyond the Standard Model in events with large b-jet multiplicity using the ATLAS detector at the LHC. European Physical Journal C, 2021, 81, 1.	3.9	5

#	Article	IF	CITATIONS
433	Measurement of the inclusive isolated-photon cross section in pp collisions at \$\$ sqrt{s} \$\$ = 13 TeV using 36 fbâ^1 of ATLAS data. Journal of High Energy Physics, 2019, 2019, 1.	4.7	5
434	Aerodynamic optimization of a morphing UAV with variable sweep and variable span. WIT Transactions on Information and Communication Technologies, 2015, , .	0.0	5
435	Prognostic value of HER2 expression levels for upper tract urothelial carcinoma Journal of Clinical Oncology, 2022, 40, 557-557.	1.6	5
436	The ATLAS inner detector trigger performance in pp collisions at 13ÂTeV during LHC Run 2. European Physical Journal C, 2022, 82, 1.	3.9	5
437	A phase II clinical trial of camrelizumab (CAM, an IgG4 antibody against PD-1) combined with apatinib (APA, a VEGFR-2 tyrosine kinase inhibitor) and temozolomide (TMZ) as the first-line treatment for patients (pts) with advanced acral melanoma (AM) Journal of Clinical Oncology, 2022, 40, 9508-9508.	1.6	5
438	Search for low-scale gravity signatures in multi-jet final states with the ATLAS detector at s = 8 \$\$ sqrt{s}=8 \$\$ TeV. Journal of High Energy Physics, 2015, 2015, 1.	4.7	4
439	Measurement of jet activity in top quark events using the ell¼ final state with two b-tagged jets in pp collisions at s = 8 \$\$ sqrt{s}=8 \$\$ TeV with the ATLAS detector. Journal of High Energy Physics, 2016, 2016, 1.	4.7	4
440	Search for excited electrons singly produced in proton–proton collisions at \$\$sqrt{s} ~=~13~ext {Te}ext {V}\$\$ with the ATLAS experiment at the LHC. European Physical Journal C, 2019, 79, .	3.9	4
441	Prognostic role of NRAS isoforms in Chinese melanoma patients. Melanoma Research, 2019, 29, 263-269.	1.2	4
442	Search for direct production of electroweakinos in final states with missing transverse momentum and a Higgs boson decaying into photons in pp collisions at \$\$ sqrt{s} \$\$ = 13 TeV with the ATLAS detector. Journal of High Energy Physics, 2020, 2020, 1.	4.7	4
443	Measurement of hadronic event shapes in high-pT multijet final states at \$\$ sqrt{s} \$\$ = 13 TeV with the ATLAS detector. Journal of High Energy Physics, 2021, 2021, 1.	4.7	4
444	Adjuvant anti-PD-1 ab (Toripalimab) versus high-dose IFN-a2b in resected mucosal melanoma: A phase randomized trial Journal of Clinical Oncology, 2021, 39, 9573-9573.	1.6	4
445	Search for top squarks in events with a Higgs or Z boson using 139Âfb\$\$^{-1}\$\$ of pp collision data at \$\$sqrt{s}=13\$\$ÂTeV with the ATLAS detector. European Physical Journal C, 2020, 80, 1.	3.9	4
446	Comments on Chinese guidelines for diagnosis and treatment of melanoma 2018 (English version). Chinese Journal of Cancer Research: Official Journal of China Anti-Cancer Association, Beijing Institute for Cancer Research, 2019, 31, 740-741.	2.2	4
447	Measurement of \$\$K_S^0\$\$ and \$\$Lambda ^0\$\$ production in \$\$t ar{t}\$\$ dileptonic events in pp collisions at \$\$sqrt{s} =\$\$ 7 TeV with the ATLAS detector. European Physical Journal C, 2019, 79, 1.	3.9	4
448	Measurement of the energy response of the ATLASÂcalorimeter to chargedÂpions from \$\$W^{pm }ightarrow au ^{pm }(ightarrow pi ^{pm }u _{au })u _{au }\$\$ events in RunÂ2 data. European Physical Journal C, 2022, 82, 1.	3.9	4
449	Systemic Therapy in Patients With Metastatic Xp11.2 Translocation Renal Cell Carcinoma. Clinical Genitourinary Cancer, 2022, 20, 354-362.	1.9	4
450	Measurement of the production cross section of pairs of isolated photons in pp collisions at 13 TeV with the ATLAS detector. Journal of High Energy Physics, 2021, 2021, 1.	4.7	4

#	Article	IF	CITATIONS
451	Search for exotic decays of the Higgs boson into long-lived particles in pp collisions at \$\$ sqrt{s} \$\$ = 13 TeV using displaced vertices in the ATLAS inner detector. Journal of High Energy Physics, 2021, 2021, 1.	4.7	4
452	Improved sliding mode guidance law based on fuzzy variable coefficients strategy. Aeronautical Journal, 2014, 118, 435-451.	1.6	3
453	Measurement of the k t splitting scales in Z → â,,"â,," events in pp collisions at s = 8 \$\$ sqrt{s}=8 \$\$ TeV with the ATLAS detector. Journal of High Energy Physics, 2017, 2017, 1.	4.7	3
454	Measurement of distributions sensitive to the underlying event in inclusive Z boson production in pp collisions at \$\$sqrt{s}\$\$ = 13 TeV with the ATLAS detector. European Physical Journal C, 2019, 79, 1.	3.9	3
455	Measurements of inclusive and differential cross-sections of combined \$\$ toverline{t}gamma \$\$ and tWl³ production in the el¹¼ channel at 13 TeV with the ATLAS detector. Journal of High Energy Physics, 2020, 2020, 1.	4.7	3
456	Measurement of isolated-photon plus two-jet production in pp collisions at \$\$ sqrt{s} \$\$ = 13 TeV with the ATLAS detector. Journal of High Energy Physics, 2020, 2020, 1.	4.7	3
457	Real-world analysis of clinicopathological characteristics, survival rates, and prognostic factors in patients with melanoma brain metastases in China. Journal of Cancer Research and Clinical Oncology, 2021, 147, 2731-2740.	2.5	3
458	Measurement of single top-quark production in association with a W boson in the single-lepton channel at \$\$sqrt{s} = 8,ext {TeV}\$\$ with the ATLAS detector. European Physical Journal C, 2021, 81, 1.	3.9	3
459	Measurement of the inclusive jet cross-section in proton-proton collisions at (sqrt{s}=7) TeV using 4.5 fbâ^'1 of data with the ATLAS detector. , 2015, 2015, 1.		3
460	Study of the spin and parity of the Higgs boson in diboson decays with the ATLAS detector. , 2015, 75, 1.		3
461	ATLAS Run 1 searches for direct pair production of third-generation squarks at the Large Hadron Collider. , 2015, 75, 1.		3
462	Measurement of b-quark fragmentation properties in jets using the decay B± → J/Ĩ^K± in pp collisions at \$\$ sqrt{s} \$\$ = 13 TeV with the ATLAS detector. Journal of High Energy Physics, 2021, 2021, 1.	4.7	3
463	A search for an excited muon decaying to a muon and two jets inppcollisions at \$sqrt{s};=;8;{m{TeV}}\$ with the ATLAS detector. New Journal of Physics, 2016, 18, 073021.	2.9	2
464	Apatinib in combination with camrelizumab, a humanized immunoglobulin G4 monoclonal antibody against programmed cell death-1, in patients with metastatic acral melanoma Journal of Clinical Oncology, 2021, 39, 9539-9539.	1.6	2
465	Four-year survival follow-up of toripalimab (JS001) as salvage therapy in Chinese melanoma patients Journal of Clinical Oncology, 2021, 39, e21522-e21522.	1.6	2
466	Search for new phenomena in final states with an energetic jet and large missing transverse momentum in pp collisions at (sqrt{s}=8~)TeV with the ATLAS detector. , 2015, 75, 1.		2
467	Tumor growth rate as an early indicator of the efficacy of anti-PD-1 immunotherapy in advanced melanoma Journal of Clinical Oncology, 2019, 37, e21050-e21050.	1.6	2
468	Search for exotic decays of the Higgs boson into b\$\$ overline{b} \$\$ and missing transverse momentum in pp collisions at \$\$ sqrt{s} \$\$ = 13 TeV with the ATLAS detector. Journal of High Energy Physics, 2022, 2022, 1.	4.7	2

#	Article	lF	CITATIONS
469	Measurement of the energy asymmetry in \$\$t{ar{t}}j\$\$ production at \$\$13,\$\$TeV with the ATLAS experiment and interpretation in the SMEFT framework. European Physical Journal C, 2022, 82, .	3.9	2
470	Analysis of overall survival (OS) and relapse-free-survival (RFS) in the phase 1b clinical trial of anti–PD-1 ab (toripalimab) plus intralesional injection of OrienX010 in stage ⣠melanoma with liver metastases Journal of Clinical Oncology, 2022, 40, 9551-9551.	1.6	2
471	Adjuvant temozolomide plus cisplatin versus high-dose interferon alpha-2b in resected mucosal melanoma: A randomized, multicenter, controlled, phase III trial Journal of Clinical Oncology, 2022, 40, 9578-9578.	1.6	2
472	Toripalimab plus axitinib versus toripalimab or axitinib alone in patients with treatment-naive unresectable or metastatic mucosal melanoma: Interim results from a randomized, controlled, phase II trial Journal of Clinical Oncology, 2022, 40, 9512-9512.	1.6	2
473	Clinical significance of CCNE1 copy number gain in acral melanoma patients. Melanoma Research, 2021, Publish Ahead of Print, 352-357.	1.2	1
474	Adjuvant radiotherapy plus systemic chemotherapy in resected head and neck mucosal melanoma Journal of Clinical Oncology, 2021, 39, e18042-e18042.	1.6	1
475	Discrepancies in response and immune-related adverse events (irAE) of anti-PD-1 monotherapy between races and primary sites in patients (pts) with advanced nonacral cutaneous melanoma (NACM) Journal of Clinical Oncology, 2021, 39, 9530-9530.	1.6	1
476	Search for heavy resonances decaying into a W or Z boson and a Higgs boson in final states with leptons and b-jets in 36 fbâ^'1 of (sqrt{s}=13) TeV pp collisions with the ATLAS detector. , 2018, 2018, 1.		1
477	Search for production of (WW/WZ) resonances decaying to a lepton, neutrino and jets in (pp) collisions at (sqrt{s}=8) TeV with the ATLAS detector. , 2015, 75, 1.		1
478	Measurement of the charge asymmetry in top-quark pair production in the lepton-plus-jets final state in pp collision data at (sqrt{s}=8,mathrm TeV{}) with the ATLAS detector. , 2016, 76, 1.		1
479	Measurement of the W-boson mass in pp collisions at (sqrt{s}=7, hbox {TeV}) with the ATLAS detector. , 2018, 78, 1.		1
480	Search for doubly charged Higgs boson production in multi-lepton final states with the ATLAS detector using proton–proton collisions at (sqrt{s}=13,ext {TeV}). , 2018, 78, 1.		1
481	A randomized phase II study evaluating the activity of bevacizumab in combination with carboplatin plus paclitaxel in patients with previously untreated advanced mucosal melanoma (NCT02023710) Journal of Clinical Oncology, 2019, 37, 9521-9521.	1.6	1
482	Mucosal melanoma of the female genital tract: Operation modalities Journal of Clinical Oncology, 2019, 37, e21060-e21060.	1.6	1
483	Surgical Outcomes of Vaginal or Cervical Melanoma. Frontiers in Surgery, 2021, 8, 771160.	1.4	1
484	Impact of different HER2 expression levels on the outcomes of second-line immunotherapy for metastatic urothelial carcinoma Journal of Clinical Oncology, 2022, 40, 524-524.	1.6	1
485	FMRP ligand circZNF609 destabilizes RAC1 mRNA to reduce metastasis in acral melanoma and cutaneous melanoma. Journal of Experimental and Clinical Cancer Research, 2022, 41, 170.	8.6	1
486	Atezolizumab plus bevacizumab in patients with unresectable or metastatic mucosal melanoma: A multicenter, open-label, single-arm phase 2 study Journal of Clinical Oncology, 2022, 40, 9525-9525.	1.6	1

#	Article	IF	CITATIONS
487	A phase Ia/Ib study evaluating the safety and efficacy of intratumorally administrated OH2, an oncolytic herpes simplex virus 2, in unresected stage IIIC to IV melanoma patients Journal of Clinical Oncology, 2022, 40, e21537-e21537.	1.6	1
488	Assessment of a HER-2 scoring system and its correlation of HER2-targeting antibody-drug conjugate therapy in urothelial carcinoma Journal of Clinical Oncology, 2022, 40, 4572-4572.	1.6	1
489	Phase Ib study of anti-PD-L1 monoclonal antibody socazolimab in combination with nab-paclitaxel as first-line therapy for advanced urothelial carcinoma Journal of Clinical Oncology, 2022, 40, 4563-4563.	1.6	1
490	Response to: Polymorphism within the 3'-untranslated region of denticleless E3 ubiquitin protein ligase homolog and survival in acral melanoma. European Journal of Cancer, 2020, 124, 65-66.	2.8	0
491	ASO Author Reflections: Primary Site Should Be Regarded as One Important Factor for Risk Stratification in Acral Melanoma. Annals of Surgical Oncology, 2020, 27, 3486-3487.	1.5	0
492	Clinicopathologic features of Xp11.2 translocation renal cell carcinoma and its response to target therapy Journal of Clinical Oncology, 2021, 39, e16559-e16559.	1.6	0
493	Second-line (2L) pembrolizumab (pembro) in Chinese patients (pts) with advanced melanoma: Three-year follow up (FU) of the phase 1 KEYNOTE-151 study Journal of Clinical Oncology, 2021, 39, e21511-e21511.	1.6	0
494	Continuous intravenous infusion Rh-endostatin in combination with dacarbazine and cisplatin as the first-line therapy for metastatic melanoma Journal of Clinical Oncology, 2019, 37, e21007-e21007.	1.6	0
495	Safety Profile of Immunotherapy Combined With Antiangiogenic Therapy in Patients With Melanoma: Analysis of Three Clinical Studies. Frontiers in Pharmacology, 2021, 12, 747416.	3.5	Ο
496	Recombinant humanized Anti-PD-1 monoclonal antibody toripalimab in patients with metastatic urothelial carcinoma (POLARIS-03 study): Two-year survival update and biomarker analysis Journal of Clinical Oncology, 2022, 40, 508-508.	1.6	0
497	Systemic therapy in patients with metastatic Xp11.2 translocation renal cell carcinoma Journal of Clinical Oncology, 2022, 40, 341-341.	1.6	0
498	Clinical characteristics of patients with collecting duct carcinoma Journal of Clinical Oncology, 2022, 40, 297-297.	1.6	0
499	Systemic treatment of cutaneous and mucosal melanoma. Chinese Clinical Oncology, 2014, 3, 25.	1.2	0
500	ASO Visual Abstract: An Evidence-Based Staging System for Mucosal Melanoma: a Proposal. Annals of Surgical Oncology, 2022, , .	1.5	0
501	The association of Ki67 level and adjuvant treatment options in mucosal melanoma Journal of Clinical Oncology, 2022, 40, e21582-e21582.	1.6	0
502	Phase Ib study of anlotinib in combination with anti-PD-L1 ab (TQB2450) in patients with advanced acral melanoma Journal of Clinical Oncology, 2022, 40, e21543-e21543.	1.6	0
503	A phase I dose-escalation study of HBM4003, an anti-CTLA-4 heavy chain only monoclonal antibody, in combination with toripalimab in advanced melanoma and other solid tumors Journal of Clinical Oncology, 2022, 40, e14586-e14586.	1.6	0
504	Toripalimab (anti-PD-1) monotherapy as a second-line treatment for patients with metastatic urothelial carcinoma (POLARIS-03): Two-year survival update and biomarker analysis Journal of Clinical Oncology, 2022, 40, 4566-4566.	1.6	0